REPUBLIC OF TÜRKİYE

ALTINBAŞ UNIVERSITY

Institute of Graduate Studies

Mechanical Engineering

DEVELOPMENT AND EVALUATION OF DRONE BASED SPRAYING SYSTEM FOR PRECISION AGRICULTURE APPLICATIONS

Ayoub EL YOUSFI

Master's Thesis

Supervisor

Asst. Prof. Dr. Yaser ALAIWI

İstanbul, 2024

DEVELOPMENT AND EVALUATION OF DRONE BASED SPRAYING SYSTEM FOR PRECISION AGRICULTURE APPLICATIONS

Ayoub EL YOUSFI

Mechanical Engineering

Master's Thesis

ALTINBAŞ UNIVERSITY

2024

The thesis titled DEVELOPMENT AND EVALUATION OF DRONE BASED SPRAYING SYSTEM FOR PRECISION AGRICULTURE APPLICATIONS prepared by AYOUB EL YOUSFI and submitted on 04/06/2024 has been **accepted unanimously** for the degree of Master of Science in Mechanical Engineering

____

Asst. Prof. Dr. Yaser ALAIWI
Supervisor

Thesis Defense Committee Members:

Asst. Prof. Dr. Yaser ALAIWI	Department of Mechanical Engineering University	________________
Asst. Prof. Dr. Abdullahi Abdu IBRAHIM	Department of Computer Engineering University	________________
Asst. Prof. Dr. Haydar İzzettin KEPEKÇI	Department of Mechatronics Engineering University	________________

I hereby declare that this thesis meets all format and submission requirements for a Master's thesis.

I hereby declare that all information/data presented in this graduation project has been obtained in full accordance with academic rules and ethical conduct. I also declare all unoriginal materials and conclusions have been cited in the text and all references mentioned in the Reference List have been cited in the text, and vice versa as required by the abovementioned rules and conduct.

Ayoub EL YOUSFI

Signature

DEDICATION

I dedicate this work to my teacher, whose unwavering support, guidance, and provision of information have been instrumental in its completion. Their assistance has helped me grasp the intricacies of drones in agriculture, a field I deeply yearn to understand from the depths of my heart.

ABSTRACT

DEVELOPMENT AND EVALUATION OF DRONE BASED SPRAYING SYSTEM FOR PRECISION AGRICULTURE APPLICATIONS

EL YOUSFI, Ayoub

M.Sc., Mechanical Engineering, Altınbaş University,

Supervisor: Asst. Prof. Dr. Yaser ALAIWI

Date: June / 2024

Pages: 103

Unmanned aerial vehicles (UAVs), also known as drones, are increasingly used for various purposes such as photography, surveillance, mapping, inspection, and agriculture. This research specifically focuses on agricultural drones, which have the potential to address challenges encountered by farmers, ultimately positively affecting crop yields. Their ability to apply pesticides accurately and autonomously, without direct human involvement, is crucial for modern farming practices. This study aims to design and simulate a quadcopter specifically tailored for pesticide spraying. The design process involves careful selection of components and simulation using both SolidWorks and MATLAB Simulink. In SolidWorks, forces are applied to the frame to assess its durability, while MATLAB Simulink is used to simulate trajectory tracking using PID controllers. The drone is engineered for precision agricultural applications, aiming to revolutionize spraying techniques by targeting specific areas in the field based on data analysis. By pinpointing exact locations requiring treatment, this approach minimizes pesticide and water usage while maximizing profitability. The research focuses on evaluating the quadcopter's performance and trajectory accuracy, offering valuable insights into its potential agricultural impact, and assisting farmers in enhancing their profits.

Keywords: Quadcopter, UAV, PID Controller, Agricultural, Precision, Trajectory Tracking.

ÖZET

HASSAS TARIM UYGULAMALARI İÇİN DRONE TABANLI PÜSKÜRTME SİSTEMİNİN GELİŞTİRİLMESİ VE DEĞERLENDİRİLMESİ

EL YOUSFI, Ayoub

Yüksek Lisans, Mekanik Mühendisliği, Altınbaş Üniversitesi,

Danışman: Yrd. Doç. Dr. Yaser ALAWI

Date: Haziran / 2024

Sayfa: 103

İnsansız hava araçları (İHA) olarak da bilinen insansız hava araçları, fotoğrafçılık, gözetim, haritalama, denetim ve tarım gibi çeşitli amaçlar için giderek daha fazla kullanılmaktadır. Bu araştırma, çiftçilerin karşılaştığı zorlukları ele alma potansiyeline sahip olan tarım dronlarına odaklanmaktadır ve nihayetinde ürün verimliliği üzerinde olumlu etkiler yaratmaktadır. Pestisitleri doğru ve otonom bir şekilde, doğrudan insan müdahalesi olmadan uygulama yetenekleri, modern tarım uygulamaları için çok önemlidir. Bu çalışma, özellikle pestisit püskürtme amacıyla tasarlanmış bir dört rotorlu drone tasarlamayı ve simüle etmeyi amaçlamaktadır. Tasarım süreci, bileşenlerin dikkatli bir şekilde seçilmesini ve SolidWorks ve MATLAB Simulink kullanılarak yapılan simülasyonları içerir. SolidWorks'te çerçeveye kuvvetler uygulanarak dayanıklılığı değerlendirilirken, MATLAB Simulink'te PID kontrolörleri kullanılarak yörünge takibi simüle edilir. Drone, hassas tarım uygulamaları için mühendislik yapılmıştır ve veriye dayalı olarak tarladaki belirli alanları hedef alarak püskürtme tekniklerini devrim niteliğinde değiştirmeyi amaçlamaktadır. Bu yaklaşım, tedavi gerektiren alanların belirlenmesi yoluyla pestisit ve su kullanımını en aza indirirken, karlılığı maksimize eder. Araştırma, dört rotorlu dronun performansını ve yörünge doğruluğunu değerlendirmeye odaklanarak, tarımsal etkisi hakkında değerli bilgiler sunmakta ve çiftçilere kârlarını artırmada yardımcı olmaktadır.

Anahtar Kelimeler: Drone, İHA, PID Kontrolör, Tarım, Hassasiyet, Yörünge Takibi.

TABLE OF CONTENTS

Pages

LIST OF TABLES

Pages

LIST OF FIGURES

Pages

ABBREVIATIONS

BLDC	:	Brushless Direct Current
COG	:	Centre of Gravity
DGPS	:	Differential Global Positioning System
EASA	:	European Union Aviation Safety Agency
ESC	:	Electronic Speed Control
GCS	:	Ground Control System
GIS	:	Geographic Information System
GPS	:	Global Positioning System
HALE	:	High Altitude, Long Endurance
LALE	:	Low Altitude, Long Endurance
LED	:	Light Emitting Diodes
LiDAR	:	Light Detection and Ranging
LIPO	:	Lithium Polymer
MALE	:	Medium Altitude, Long Endurance
MAV	:	Micro or Nano Air Vehicles
MEMS	:	Orthogonal Frequency Division Multiplexing
MTOW	:	Maximum Take-off Weight
NIR	:	Near Infrared Band
ONEU	:	North-East-Up
PC	:	Personal Computer
PF	:	Precision Farming
PF	:	Precision Farming

RED:	:	Reflectance of the Red Band
RGB	:	Red Green Blue
RPAS	:	Personal Area Network
RPAS	:	Remotely Piloted Aircraft System
RPM	:	Rotations Per Minute
RPV	:	Remotely Piloted Vehicle
UAS	:	Unmanned Aircraft System
UGV	:	Unmanned Ground Vehicles
USDA	:	United States Department of Agriculture
VTOL	:	Vertical Take-Off & Landing
WHO	:	World Health Organization)

LIST OF SYMBOLS

λ	:	Linear Position
η	:	Euler Angles
V1	:	Linear Velocities in the Inertial Frame
ω_E	:	Euler Angle Rates in the Inertial Frame
$R_z(\psi)$	:	Rotation Matrix for Rotation about Z-Axis.
$R_y(\theta)$	:	Rotation Matrix for Rotation about Y-Axis.
$R_x(\varphi)$	:	Rotation Matrix for Rotation about X-Axis.
R_I^B	:	Rotation from a Body-Fixed B Frame to an Inertial Frame I.
T_I^B	:	Euler Angles.
m	:	The Mass of Rigid Body.
F_B	:	External Force.
M_B	:	External Moment.
I	:	Moment.
F_M	:	Force Generated by Motors.
F_G	:	Force Gravitational.
F_w	:	Force Exerted by Wind.
M_M	:	Moment Generated by Motors.
M_G	:	Moment Gravitational.
M_w	:	Moment Exerted by Wind
K_p	:	Proportional Gain.
K_D	:	Derivative Gain.
K_I	:	Integral Gain.

$e(t)$: The Error Term.

$u(t)$: The Control Input.

1. INTRODUCTION

Nowadays, the world anticipates a population exceeding 9.5 billion by the year 2050 [1]. The swift population growth, increased consumption, and many signs of deteriorating the global environment have destroyed the balance between food demand and food availability [2]. Additionally, the statistics indicate an expansion in the number of people suffering from chronic hunger due to these expectations. Consequently, meeting these challenges cannot be done by using conventional farming methods. In today's world technology has change the way how the framers work in rural areas in all over the world, and that is make the gap between the demand and the technology available growing during the time especially in agriculture, that's why farmers looking for more efficient equipment to increase the productivity and meet the demand of the food. also looking for equipment that can protect the health and safety of workers who handle the spraying of harmful pesticides and fertilizers manually. The current method of manual spraying can lead to numerous adverse effects. These effects range from mild skin irritation to more severe consequences such as birth defects, tumors, genetic changes, blood and nerve disorders, endocrine disruption, and even the risk of coma or death. The WHO (World Health Organization) has even predicted that as many as one million people could be adversely affected by pesticide exposure in crop fields and that's paved the way for invention of century drones [3]. The global agriculture faces big problems like Crop diseases and pests, those are the significant factors that affect the quality and productivity of crops. To address these issues, chemical products such as pesticides are commonly used to minimize losses and improve productivity. However, it is crucial to select the appropriate equipment for the application of these chemicals. For example, in China there are more 80% of manually operated sprayers like manual air sprayer, knapsack sprayer but the quality of spraying depends on the skills of the sprayers [4]. Due to these challenges, Japan developed the first prototype of unmanned aerial vehicles spraying to cover hectares of forestry and crop in 1985. And in 1987 the first model was designed by Yamaha R-50 can hold payload with capacity 15 Kg in order to dusting the crop [5]. Commercial version was introduced to the market in 1989, because of the weight the UAV's was subject to international arms regulations due to its weight [6]. Drones or unmanned aerial vehicles are aircraft which can be autonomously piloted from a distance without the need for direct contact with drone, this minimize any potential side effect on the pilot and the farmers operating the controller [7]. All applications that assist farmers, such as spraying drones, monitoring drones, mapping drones – all these applications are now readily available in the market, equipped with all the necessary features, that's opens the possibility for fierce competition and ability for challenging the deteriorating global environment, mitigating the side effects of manual spraying, and ultimately boosting productivity also faster 40 times more than traditional farmers. As result, in 2010, the drone market was valued at approximately 4.9 billion USD. According to analytical data, the valuation of business services utilizing drones is projected to increase to roughly 127 billion USD, the agricultural sector has adopted and integrated drone technology where these advance tools utilize to modernize the way of farming [8]. The utilization of traditional farming methods has posed numerous challenges for the farmers, incurring significant cost over the years. Conservative estimates indicate that worldwide crop losses due to diseases, insects, and weeds amount to $220 billion annually, comprising 31-42% of all losses. The statistics illustrate the breakdown: diseases contribute 14.1%, insects 10.2%, and weeds 12.2% to the total average losses of 36.5% [9]. According to the statistic of Global market studies site the using of crop protection increased roughly between 2016 and 2024, the value of global market for crop protection is estimated in 2016 around 54.89 billion USD $ and is projected to reach USD 65.21 billion by 2021, growing at a CAGR of 4.45% from 2019 to 2024 [10]. Spraying drones are the latest and the most widely method used it with the crop protection among the farmers, The increasing of spraying drones is a result high of demand and efficiency of this tools also the benefit of protecting the farmers from the potential side effect of spraying manually applying crop protection measures. In agriculture pest control, we need to use methods more precision to improve the quality and increase the production rate. It's necessary to use precision pesticide spraying vehicles instead of the conventional spraying method. Spraying method divide to old method old and new tools, the first olde method dating back to the1850s in the USA in order to protect potatoes from the Colorado Beetle involving using knapsack tank without pump, so the spray was fed by gravity to two sprinklers. The first new method, initiated by Ray Hagie in 1947, marked his distinction as the first person who invent the high clearance self-propeller sprayer. After that he expanded to develop the first rear-wheel drive sprayer, which was the first to have mounted prayer boom. Precision farming is a way of managing farming that focuses on using the right number of inputs. This helps save money in crop production and reduces the impact of harmful substances on the environment. The goal is to use resources efficiently, minimize waste, and increase overall crop yield. In particular, precision farming seeks to cut down on the costs of chemicals like fertilizers and pesticides, lessen their negative effects on the environment, produce high-quality crops in large quantities, and improve the flow of information for managing crops The plant protection is the process of safeguarding plants from diseases and various pests to enhance crop yields and improve their quality [11]. To achieve this, agricultural pesticide spraying is employed as a method to protect plants from pests and diseases. In our country, plant diseases are a common factor that negatively impacts crop yields, making it challenging to fully implement the precision farming approach [12]. Developed countries use the UAV in agriculture to control agricultural lands. That's consequences big demand of this robots agricultural, The UAV usage cantered on precision farming and remote sensing applications. The purpose of sensing it is to get information about the land like growing rate diseases. For precision farming it's important to control the quality health of the crops and improve the pesticide spraying [13].

1.1 MOTIVATION

Motivation has been referred to as the single most important factor for success in research work not having certainty in the product of research study is one of the major demotivators for the researchers (Millat-e Mustafa 2005). As far as my thesis is concerned, the motivation behind this research is continuous as it is embedded in personal and professional aims and objectives. My primary motivation for this research comes from my strong desire to pursue a Ph.D. in the field of UAVs, which stands for Unmanned Aerial Vehicles. The UAV field has experienced significant growth in recent years, and it's a dynamic source of innovative ideas that keep me intellectually engaged. Before diving deep into this field, I aimed to take my academic journey to the highest level and ensure that my work has a real-world impact on both industry and the broader world. Our world relies heavily on agriculture to supply food and meet the growing global demand for both food and bioenergy. For a long time, traditional methods of crop spraying, which involved manual labour and the use of large, cumbersome machinery, have been labour-intensive and harmful to the environment. The strategies used for crop spraying have remained time-consuming and inefficient for many centuries. The use of spraying drones in agriculture is gaining popularity and attention because it promises more efficient, accurate, and environmentally friendly alternatives. I have always been motivated in this area by a desire to contribute to the development of sustainable agriculture and gain a better understanding of the challenges faced by modern agriculture. In addition to this, coming from a background closely connected to agriculture, I've had a firsthand and lively experience of its importance. I hold the well-being of farmers and the improvement of agricultural practices for them in high regard, particularly through the adoption of high-precision technology. The positive impacts of addressing these concerns are numerous. Farmers could enjoy a more relaxed farming process because they wouldn't need to work directly in the fields. This would also reduce their exposure to harmful chemicals. Moreover, the yields from crops tend to be significantly higher when compared to manual crop spraying. To sum it up, my motivation for studying drones in the agricultural context stems from my clear goal of advancing my education in the safe use of drones for farming, which is reflected in my dedication to this field. Additionally, our engagement in agriculture in Morocco ignites my passion for this topic. Finally, my commitment to staying updated with the latest information in my field of study further fuels my enthusiasm for this research.

1.2 THESIS OBJECTIVES

Drones have become pivotal in various sectors due to their effectiveness and versatility. Unmanned aerial vehicles applications are now divided into multiple sub-sectors, such as photography, mapping, agriculture, and more. Each application calls for specific types of drones. During this research I will focus on agricultural drones, starting with exploring the various types of drones, and how the drone's diversity plays roles in agriculture. This research is focused on study of quad-copter aircraft, including explanation of their operation, the requirement for selection the components based on task need such as the motor type and the size of the propeller, design in SolidWorks, modelling, and visual ideation of the agricultural drone. Each of the individual components of the agricultural drone was measured, sketched, and designed, simulation using MATLAB to simulate the agricultural drone after drawing all the component of Spraying drone in SolidWorks. Furthermore, the integration of a multispectral camera adds a crucial dimension to the project. By analysing data captured by this camera, the aim is to minimize pesticide usage while effectively controlling crop health. This strategic approach not only optimizes agricultural practices but also enhances overall profitability. The primary purpose of this agricultural drone is for spraying applications. The main objective is to integrate a tube system that connects to a large tank on the ground, facilitating an uninterrupted supply of pesticides or water to the drone. The aim is to evaluate the drone's performance while operating with this integrated tube system. Additionally, we will explore the most effective method to ensure maximum crop coverage during the spraying process.

1.3 THESIS STRUCTURE

Chapter 1: Introduction

This chapter provides an overview of the research, highlighting the significance of drones in agriculture and their potential to address challenges faced by farmers. It presents the main objectives of the study, which include designing a quadcopter for pesticide spraying using SolidWorks and MATLAB Simulink and integrating a multispectral camera for precision agriculture. The chapter also outlines the motivation behind the research and the scope of the study.

Chapter 2: Literature Review

In this chapter, a comprehensive review of relevant literature is presented, covering topics such as the historical development of unmanned aerial vehicles (UAVs), types of UAVs, spraying farming methods, precision farming, remote sensing, plant disease detection, and related work in the field of agricultural drones. The chapter aims to provide a solid foundation for understanding the current state of research and identifying gaps that this study aims to address.

Chapter 3: Methodology

This chapter describes the methodology employed in the research, including the design process of the quadcopter using SolidWorks, the selection of components based on payload estimation, and the integration of a multispectral camera. It also covers the mathematical modelling, control system design using PID controllers, and the implementation of the quadcopter in MATLAB Simulink. The chapter provides a detailed explanation of the methods used to achieve the research objectives.

Chapter 4: Results and Discussion

In this chapter, the results obtained from the numerical simulations and data analysis are presented and discussed. It includes the Simulink implementation and PID response analysis for the quadcopter's trajectory tracking, as well as the utilization of advanced data analysis and visualization tools like Pix4Dfields and Agremo for precision spraying in agriculture. The chapter also demonstrates the integration of spray control mechanisms and drone visualization in MATLAB. The results are interpreted in the context of the research objectives, and their implications for precision agriculture are discussed.

Chapter 5: Conclusion and Future Work

The final chapter summarizes the main findings and conclusions of the research, emphasizing the significance of the results in advancing the use of drones for precision agriculture. It discusses the potential impact of the study on the agricultural industry and highlights the advantages of integrating drones with multispectral cameras and advanced data analysis tools. The chapter also presents recommendations for future research, identifying areas that require further investigation to fully harness the potential of drones in agriculture.

2. LITERATURE REVIEW

2.1 HISTORICAL DEVELOPMENT OF UNMANNED AERIAL VEHICLES UAV

In today's transforming world, the need of new technologies is becoming a necessity for the big global transformation and significant demand in sources like food, military, there's many types of technology involved in every sector and one of this sector is Unmanned aerial vehicles that's becoming one of the most important technology sector that significantly contributed to time saving and enhanced productivity [15,16].

Drones are known as Unmanned aerial vehicle (UAVs) or unmanned aircraft as technical terms, also known as robot flying [16].with capability to be controlled by a human operator from a distance or operate independently, gathering data from sensors and external devices while the drone following the instructions given by the operator [15].The drones is used for application collecting data [17],military, agricultural, photography, shipping and delivery, safety inspection [16],firefighting surveillance, aerial photography and others [18].Due to their speed, accuracy and ability for carrying out different task's [19],additionally their ability for collecting data and store it until for later analysis contributes to improve performance.

In the history of drones the United states, the United kingdom, Russia, Germany were the countries that led the way in drones research's, the first time an unmanned flying vehicles was used by the Austrians was in August of 1849, during this siege, they launched the first air raids in history, by unmanned balloons which floated over Venice carrying bomb [20].

Charles Kettering collaborated with Elmer Sperrym, Orvill Wright and Robert Milikanem are develop the first Pilot-less aircraft, known as Kettering Aerial Torpedo "Kettering Bug" around 1915,it operated automatically ,based on sensors like a barometer for altitude measurement and engine's revolution for distance calculations [21]. Furthermore, drones have a historical presence, with examples like the Gipsy Moth in 1929, DH.82 Queen Bee in 1935, and Radio plan in 1939, reflecting the evolution of drone technology over different eras.

Drones have evolved significantly over time offering a range of features and capabilities that make them suitable for various tasks. This increased functionality is also a result of competition, which has led to prices making drones more accessible to a larger audience. as instance Military drones Predator MQ-9, Agricultural Drone, Photography Drone.

According to a study in February 2013, unmanned aircraft vehicles (UAVs) were utilized by over 50 countries, including Iran, China, and Turkey, which have developed their own UAVs. The United States is the sole country that has acquired over 11,000 drones specifically for military purposes. Aviation companies, academic institutions, and government researchers are eagerly working on the development of advanced aircraft, which vary in size from small robotic insects like moths and hummingbirds to larger models like Boeing's Phantom Eye [22].

The current drone market is rapidly growing up and has positive economic impact over the world, a report published by Goldman Sachs revealed that the drone market reached 100$ Billion USD in 2020, 70 billion USD represent military activity. Furthermore, the worldwide drone population is projected to grow from 5 million in 2020 to an estimated 9.6 million by 2030 [23].

Actually, the use of drone has risen over the last few decades due to their rapidly involving and divers application [24].For using the drone like disaster management provide security, application in agriculture sector (pesticide, fertilizer, monitoring..), construction sector and photography sector [25].The variety of drones application due to multiplicity of drone types, with each type designed to perform specific task's according to its form. for instance, spraying drones have multi-rotor designed to support the heavy payload they carry. This diversity is why various types of drones exist.

2.1.1 Unmanned Aerial Vehicles

A UAV, or Unmanned Aerial Vehicle, is an aircraft that operates without a human pilot on board. Utilizing inertial sensors and navigation technology, it possesses the potential to fly either remotely or independently, while taking into account predetermined flight destinations [26].

In 1915, Tesla initiated the concept of pilotless flying by proposing the employment of an armed, unmanned aircraft as a means of aerial defense for a nation. The path of flight is mainly monitored from a remote location by a ground flight control system. to quickly react in an instance of an emergency. The term UAVs (Unmanned Aerial Vehicle System) includes fixed-wing and rotary-wing UAVs, lighter-than-air UAVs such as balloons and airships, deadly aerial vehicles, decoys and targets, alternatively piloted aircraft, and uninhabited combat aerial vehicles [27].

Unmanned aircraft can be classified based on various criteria like MTOW (Maximum Take Off Weight), size, features of aerodynamics ,and number of the rotor [28]. In this section we will focus on the type of rotor, because of its importance in the agriculture sector, as it holds particular significance in the agriculture sector.

To differentiate these robot aircraft from other types of ballistic missiles, balloons, blimps, and projectiles, the term "Unmanned Aerial Vehicle" (UAV) became popular in the 1990s. Since then, the UAV has gone by many different names: UAS, RPV (for the United States Air Force), RPAS (for the United Kingdom), and drones [29].EUROCONTROL, EASA, and FAA, which are important international organizations, have recently embraced the term unmanned aircraft system (UAS) as the appropriate official terminology. The alterations in the acronym are attributed to the following factors. UAS stands for Unmanned Vehicles Systems, and the expression unmanned indicates that these vehicles operate without a pilot physically present on board. The term aircraft refers to a type of vehicle that is capable of being deemed airworthy. The term system refers to a comprehensive entity that encompasses not only the flying aircraft itself, but also includes a Ground Control System (GCS), communication units, and take-off and landing systems. A typical Unmanned Aircraft System (UAS) consists of system components divided into three main divisions.

2.2 UAS PLATFORM TYPE AND CLASSIFICATION

2.2.1 UAV Platform

UAV Platform is an aircraft which can flight without human intervention, and can be controlled distantly with radio channel, UAV can be categorized according to the number of the rotor in integrated into their platform, and those are the type of model’s UAV aircraft are used in last two decade, there’s three main type of UAVs platforms, Fixed wing, Helicopter and Multi-copter [30].

2.2.2 Fixed Wing

The term fixed wing is frequently used in the aviation industry to refer to specific types of aircraft. These planes have wings. To fly, you must have enough forward airspeed to provide the necessary lift. The wings of fixed wing aircraft are stationary, in contrast to rotating wing helicopters or drones.

2.2.3 Single Rotor

Single-rotor helicopter drones are equipped with a solitary rotor to maintain flight and a tail rotor to manage its direction. The advantages of this aircraft are its ability to do VTOL

(Vertical Take-off and Landing) and hover flying, its extended endurance (which may be achieved by using gas as a power source), and its higher payload capacity. Drawbacks encompass increased complexity in piloting and the requirement for further training. These devices are commonly employed for conducting airborne LiDAR laser scanning [34,35].

2.2.4 Multi-Rotor

Multirotor systems fall under the category of rotorcraft which refers to aircraft that use rotating wings for lift. It's popular because of their mechanical simplicity when compared to the helicopter [33]. Rotorcraft can have one or multiple rotors. Drones, with systems typically have small rotors to ensure stability hence they are called multirotor systems. These drones are commonly utilized at four rotors, for flight. For instance, a multirotor system that consists of more than two rotors with configurations like quadcopters, hexacopters, and octocopters [34].

2.3 TYPES OF UNMANNED AERIAL SYSTEMS

Six distinct categories of UAS platforms are classed based on their flying altitude and endurance limitations. The following are the types of Unmanned Aerial Systems (UAS) [35].

a. MAV (Micro or Nano Air Vehicles) Military aircraft, renowned for their compact dimensions, are commonly brought in backpacks and operate at low altitudes (330), with brief flight durations ranging from 5 to 30 minutes.
b. VTOL (Vertical Take-Off & Landing) Unmanned aerial vehicles (VTOLs) are specialized aircraft used in situations where terrain limitations require specialized capability. They operate at low altitudes and have high power requirements for hovering flight, except in larger sizes.
c. LASE (Low Altitude, Short-Endurance) Small unmanned aircraft systems (sUAS) eliminate runways and require lightweight, wingless aircraft for easy field deployment, recovery, and transport. However, these systems often have limited endurance and communication ranges.

d. LALE (Low Altitude, Long Endurance) UAS, typically at the upper end of the FAA's "UAS" weight designation, can hold many kgs at altitudes of a few thousand meters for extended periods.
e. MALE (Medium Altitude, Long Endurance) Aircraft are typically larger than low-altitude UAVs. They operate at altitudes of up to 9,000 m and may fly hundreds of kilometres away from their base stations for extended durations.

f. HALE (High Altitude, Long Endurance) HALE aircraft are the largest and most complex UAS, capable of flying at altitudes of 20,000m on thousands of km missions, with some lasting over 30 hours [36].

In the realm of diverse UAV classifications, the significance of Vertical Take-Off & Landing (VTOL) systems stands out notably. VTOL UAVs, specialized for terrain-restricted operations, offer crucial capabilities for missions requiring flexible manoeuvrability and accessibility. These UAVs, particularly efficient in overcoming terrain limitations and operating at low altitudes, accommodate high power demands, especially during hovering. Their adaptability and ability to navigate confined spaces make VTOL systems an asset in various fields, including agriculture, military, logistics, Etc.

2.4 SPRAYING FARMING METHOD

In order to protect plants, using non-chemical methods there are alternative solutions such as cultivation for pest and weed control, biological applications for pest control, mechanical and laser cutting applications for weed control [37]. Currently, pesticide spraying has become the primary method used in plant protection applications. Conventional methods for pesticide spraying are commonly adopted in agriculture. The spraying methods may be classified into three categories: ground vehicles, aerial vehicles, and hand spray machines [38].

2.4.1 Ground Vehicles

Ground vehicles are often preferred for pesticide spraying due to their significant carrying capacity and extensive spraying ranges. However, the average weight of modern agricultural machinery, which can exceed 80,000 pounds, surpasses even that of the heaviest living terrestrial animals. While this extra weight enhances the power and efficiency of machines, it also leads to soil compaction, squeezing out air and compressing the land. This compaction impedes root development, nutrient uptake, and renders the land more susceptible to flooding and erosion. The intensification of modern food production, coupled with efficient agrotechnical practices, poses a growing threat to soil structure and the long-term productivity of arable land. Researchers Thomas Keller of the Swedish University of Agricultural Sciences and Dani of the Desert Research Institute modelled the forces exerted by tires on the soil at various depths, considering the varying weights of agricultural machinery. They observed that subsoil stresses under farm vehicles have affected progressively deeper soil layers over the past six decades, potentially encroaching upon untilled crop root zones. The increasing weight of agricultural machinery suggests that an emphasis on efficiency, floatation, and traction may have overlooked intrinsic soil limits. It is imperative that future agricultural vehicles be designed with these intrinsic soil mechanical limits in mind to mitigate chronic soil compaction [39].

2.4.2 Hand Spray

Conventional farmers commonly resort to hand spray equipment for pesticide application, but this method proves inefficient when dealing with extensive farmland. Research reveals that pesticide exposure and a lack of protective gear significantly contribute to illnesses among over 75% of Cambodian migrant labourers in Thailand. Shockingly, more than 80% of surveyed workers were found to be wearing inadequate attire, offering insufficient protection against chemical exposure. The use of backpack sprayers, which emit exceedingly fine particles, exacerbates the risk. Additionally, migrant laborers in Thailand who encounter pesticides may lack health-screening measures and often forego protective gear due to language barriers. The authors of the study recommend familiarizing workers with Thailand before their relocation and providing comprehensive health education to address these challenges [40].

2.4.3 Aerial Vehicles

An alternate method for long-distance pesticide spraying is the use of a piloted aerial vehicle. Due to their required safe flying altitude, these vehicles are unable to spray pesticides closer to the plant. Drift induced by airplanes due to flying height and wind reduces the efficacy of pesticide treatments. It is expensive since it requires highly trained pilots. While spraying is an essential element of farming, doing it by hand requires a lot of time and energy and uses chemicals that may be harmful to humans. Drones offer more precision than human workers for treating diseased plants. Farmers may plot flight paths over the regions that need spraying, and doses can be programmed to predetermined values, eliminating waste and keeping farmland free of excessive chemical residue, hence lowering pollution levels and improving the safety of the food produced there [41]. Traditional methods for preventing the propagation of pests and illnesses in agricultural areas are insufficient. It's apparent that utilizing traditional spraying methods reduces crop output efficiency [42]. Particularly, the excessive use of chemicals in these approaches has a deleterious effect on soil, plants, and plant roots in agricultural areas. Additionally, traditional approaches are not viable options for precision farming.

2.5 PRECISION FRAMING

To enhance resource usage efficiency, productivity, quality, profitability, and sustainability in agricultural production, precision agriculture is a management method that makes use of data. To make judgments based on estimated variability, it is necessary to combine data at the temporal, geographical, and individual levels. In order to control the amount of water, seed, and fertilizer used in a crop, precision farmers implement techniques such as site-specific nutrient management, remote sensing, global information systems, and variable rate applications. By tailoring inputs and procedures to specific crops and agro-climatic conditions, this method strives to boost yield, quality, profit, decrease waste, and become environmentally friendly [43]. The fundamental principle behind precision farming is the application of different technological resources that reduce potential risks to soil, environment, and human health. Finding, measuring, and controlling variables are essential for precision farming [44]. Advanced agricultural utilization rates vary widely across countries and regions. In a survey from 1998, just 15% of British farmers reported using precision agricultural technologies [45]. Daberkow and McBride (2000) analysed the results of the USDA's 1998 Agricultural Resource Management Study survey and found that the Midwest (heartland) had the highest adoption rate for corn and soybeans and the South had the lowest. While 1.6% of animal farmers have adopted precision farming techniques, 13.7% of grain and oil seed farmers have. At 5.8 percent, the Northern Great Plains area was the second-fastest in the United States to embrace precision agricultural technology. Some of the country's early adopters are said to call this area home because of its enormous farm sizes and very short producing seasons.

2.5.1 Advantages Of Precision Farming

PF has several benefits, including the ones listed below [46].

a. In the precision farming concept, all potential growth-related issues are figured out by regular, one-by-one inspections of crop plants and data management.
b. This method of crop improvement is far more efficient, straightforward, and precise. Precision farming makes soil mapping and analysis simple.
c. Precision farming is an innovative technique used in agriculture that helps farmers save money by reducing the number of resources wasted.
d. Data management allows for the accurate utilization of necessary requirements.

2.5.2 Disadvantages Of Precision Farming

Precision farming has many advantages but also some problems including expensive startup costs, the need for specialized knowledge, and technological reliance. Disruptions to farming activities caused by technical problems can be costly. Unauthorized access to confidential information is another major security risk. Furthermore, the rural-urban gap may be exacerbated since not all farmers have access to or can afford sophisticated technologies. Consequently, there are advantages and disadvantages to precision farming [47].

2.6 REMOTE SENSING

By mapping crop and soil variability, remote sensing facilitates effective monitoring of environmental factors that impact plant health, production, and quality. It's utilized in GIS analysis to help direct field samplings, make sense of trends, and decide how to manage things now and in the future. Remote sensing may be used in tandem with other management tools such as crop simulation models to shed light on the past and foretell the future. Since NIR reflectance is closely connected with yield, a field's behaviour in yield terms may be seen by a temporal study of RS data [48].

Since the debut of soil organic matter sensors, remote sensing applications in precision agriculture have evolved to include satellite, aerial, and handheld sensors. Light detection and ranging (LiDAR), fluorescence spectroscopy, and thermal spectroscopy are just a few examples of the cutting-edge applications made possible by the widespread usage of electromagnetic radiation across a wider range of wavelengths. Improved study of individual chemicals, molecular interactions, crop stress, and biophysical features is now possible with hyper-spectral remote sensing because of its narrower spectral bandwidth. The field of precision agriculture now has access to a wide range of spectral indices. With the improvement in spatial resolution of aerial and satellite photography from hundreds of meters to sub-meter accuracy, soil and crop attributes can now be evaluated with high precision. Similarly, the temporal frequency has increased [49].

Agricultural remote sensing employs various tools, including satellites, airplanes, tractors, and handheld sensors, to capture reflected radiation from soil or plants without directly interfering with them. This technique allows for the measurement of radiation levels in farmland. Apart from analysing reflectance, transmission, and absorption, it also considers the release of energy through fluorescence from plant leaves [50], and thermal emission [51].

2.6.1 Remote Sensing Platforms

Data for Earth Observation is collected by satellites and aerial platforms, with satellites providing multispectral imagery but with short revisit times. Multispectral and hyperspectral photos may be captured on demand by airborne vehicles, giving more freedom but also greater expenses. UAVs (drones) are rapidly gaining popularity for remote sensing due to their decreased price and increased availability. High-resolution digital elevation models are only one example of the many technological advances made in the UAV industry since its inception in the late 1970s. The usage of unmanned aerial vehicles (UAVs) has increased in recent years, with these vehicles collecting EO data for a wide range of purposes, including agriculture, environmental monitoring, disaster management, and scientific study [52]. Integrating Unmanned Aerial Vehicles (UAVs) with remote sensing technology is a strategic approach for collecting spatial data on land cover, natural resources, and the environment. UAVs have exceptional frequency and resolution capabilities, allowing for multiple deployments and high-definition data collection. These technologies enhance Earth's surface understanding, aiding in land administration, farming, ecological preservation, and emergency response. The use of D-GPS for precise geolocation is crucial for monitoring environmental changes over time. [57,58] Unmanned Aerial Vehicles (UAVs) present several advantages due to their lack of human pilot constraints, ability for real-time operations, and rapid data acquisition. They find utility across various sectors, including remote sensing, aerial photography, NDVI analysis, thermal imaging, pest control, and disease surveillance in precision agriculture. However, it's important to acknowledge that UAVs come with both benefits and drawbacks across different applications, including NDVI analysis, thermal imaging, pest control, and disease surveillance.

2.7 PLANT DISEASE DETECTION

Most commercially available solutions for detecting plant diseases use a combination of light emitting diodes (LED) and photodiodes in an electronic circuit, but they often lack efficiency in detecting plant diseases. These LED-based sensors struggle to differentiate between healthy and diseased plants, limiting their usefulness in precision farming [55]. However, emerging technologies such as multispectral cameras offer promise in overcoming these limitations. By capturing images of plants across multiple wavelengths, multispectral cameras can provide more detailed information about plant health, allowing for better disease detection and management. Plants exhibit varying reflectance patterns across the electromagnetic spectrum, with different bands showing significant differences in reflected light intensity. This variation allows for more accurate discrimination between plants. In a study, hyperspectral analysis of weeds and crops was conducted using satellite and aerial platforms. The results showed that by increasing the number of wavelength bands from 3 to 22, the overall accuracy of classifying 6 crop species improved from 56% to 90%. Utilizing more wavelength bands in the electromagnetic spectrum, where plants exhibit distinct optical reflectance characteristics, can lead to more precise plant disease discrimination [56].

2.8 MULTISPECTRAL CAMERA

Multispectral imaging (MSI) is essentially using a full spectrum of light to get clearer distinctions between different elements in tissues. It takes pictures at different wavelengths, linking specific spectral patterns with chemical components through light absorption. MSI isn't just limited to one field; it's being used in various areas like precision farming, restoring artwork, environmental surveillance, and biochemical research. Multispectral imaging relies on a system that uses light emitting diodes (LEDs) to capture images. These LEDs emit specific narrow band spectrum lights, resulting in a series of grayscale images [57].

Multispectral imaging combines two or more spectral imaging bands within a single optical system. Contrary to hyperspectral imaging, which involves narrower bandwidths, multispectral imaging covers broader ranges. Typically, these systems combine various bands into one setup, including:

a. The visible spectrum, encompassing blue, green, and red bands (400 - 760nm).
b. Near Infrared (NIR) band (0.7 - 1 μm).
c. Short-Wave Infrared (SWIR) band (1 - 1.7 μm).
d. Mid-Wave Infrared (MWIR) band (3.5 - 5 μm).
e. Long-Wave Infrared (LWIR) band (8 - 12 μm).

2.9 CROP MONITORING

Monitoring the crop condition especially during the growth stages is essential to farmers. The details they get help them decide what to do next to make sure they get the best harvest possible. Cameras are an immense help here, and there are a few types they use a lot: digital, thermal, and multispectral. Thermal ones, with infrared sensors, make maps showing the crop's temperatures. Digital cameras give colour info by processing images, and multispectral ones take both visible and invisible pics using different light types to take a detailed picture of the crop [58].

The multispectral camera sent data through telemetry, and that information was looked at by a Geographic indicator. This indicator used something called the Normalized Difference Vegetation Index (NDVI) to analyse the data. Its method formula is utilized to assess the level of greenness in plants, as indicated by Eq 1. When calculating NDVI for a particular pixel, the resulting value always falls within the range of minus one (-1) to plus one (+1). However, values close to zero suggest an absence of greenery, while those closer to +1 (around 0.8 - 0.9) indicate the highest density of green leaves. one of the equations Used to fin [59].

2.10 ROBOTIC

Lately, there have been big advancements in robotics across various fields. It's expected that in the coming years, robotics will take over a lot of everyday and industrial tasks. This tech is super useful because it gives more movement, makes services better, and boosts how well products work. Plus, it has the power to make life and work easier, bringing a lot more comfort and changing how things get done. These days, robotics is a major force driving competitiveness and adaptability in big manufacturing industries. While service robots in fields like agriculture, transport, healthcare, security, and utilities aren't as developed yet, they're predicted to become the biggest area for robot sales worldwide [60].

A lot of economic experts think that the robotics industry could be the next big thing, just like how IT was booming in 2000. Japan figures it could hit $13.2 billion soon, and South Korea is really pushing to grow its robot industry, aiming for a huge $39.4 billion market. Both governments are betting big on robotics.

As definition of robot, A robot is like a flexible, multi-use arm that can be programmed to handle different jobs by moving things – materials, tools, or specific gadgets – in specific ways. It's a versatile machine that can do lots of different tasks based on the instructions it's given [61]. Additionally, A robot is an automatic, servo-controlled, freely programmable, multi-purpose manipulator with several degrees of freedom. Variably programmed operations make possible execution of a multiplicity of tasks [62].

Robots are great for certain jobs because they do not get tired like we do. They can manage tough or risky conditions that might be uncomfortable or unsafe for people. They work simply fine in places where there is no air. Plus, they don't get bored doing the same thing over and over, and they stay focused on the job without any distractions [63].

Robots come in different forms based on how they move around—like staying still, using wheels, legs, flying, and other types. For instance, Unmanned Ground Vehicles (UGV) belong to the wheeled robot category, while Unmanned Aerial Vehicles fall into the flying robot group.

2.11 RELATED WORK

According to the information in reference [64], Sadhana B and her team made even more improvements to the methods that were already stated. They created a quadcopter UAV with a spraying module that was made to make the use of pesticides in agricultural areas more efficient. It was the goal of this new idea to increase crop production and keep important resources safe. The quadcopter used in this project can carry up to 1 kg of cargo and is set up to spray pesticides from low altitudes. It works with Brushless Direct Current (BLDC) motors, an Electronic Speed Control (ESC) system, an MPU-6050 unit with a MEMS sensor and a MEMS gyro, a radio receiver, a LIPO battery, and the pesticides spraying module. The Arduino UNO AT mega328 controls it all. Additionally, according to reference [65], Tejas S. Kabra and a few others created a cheap and light quadcopter with the main goal of improving the arm design to make it more useful in farming. The quadcopter has a body made of lightweight metal and streamlined parts that make it easier to use and more accurate in farming. Notably, these innovative ideas also help lower the health risks that come with spraying pesticides by hand. The paper talks about important parts of the quadcopter, such as its stand, sprayer, pipe system, pesticide container, and special propellers that are all made to make spraying time better and the quadcopter lighter overall. Furthermore, Yallappa D. and his fellow students made a sprayer that can be attached to a drone. It has six Brushless Direct Current motors, a hexacopter frame, and can carry 5 kg. LiPo batteries, a pesticide tank, a pump, and a frame for support make up the set. The weight of the drone was carefully estimated by looking at things like the frame design, landing gear, fluid tank design, motor choice, battery, propellers, flight controller, transmitter, and receiver. This sprayer works well to put chemicals on rice fields and garden crops, which lowers the cost of using pesticides and protects the environment [66]. Lastly, using a GPS module and different devices, Munmun Ghosal and his team created a system that can track the amount of pollution in different places. The system, which is run by an Arduino board, figures out the air quality score by looking at data about smoke levels, CO_2 levels, temperature, light intensity, and humidity. This data is shown on an online server using Apache software, which lets people act quickly to lower health risks. The device is both efficient and cost-effective, so it can be used to check the air quality in smaller settings [67].

2.12 SPRAYING SYSTEM

A spraying drone is an autonomous aircraft utilized for accurate dispensation of chemicals such as insecticides and fertilizers in agricultural areas. The technology provides enhanced accuracy, less reliance on pesticides, and superior distribution, thereby improving the well-being and efficiency of crops. To exemplify the significance of utilizing spraying technologies, we can examine their influence in stationary scenarios. This emphasizes the importance of these instruments in different situations. According to the World Health Organization, more than 220,000 people die each year from pesticide poisoning, which affects poor countries the most. It is known that some pesticides, like organophosphates and carbonates, are bad for the nervous system [68]. Some pesticides may also irritate the skin or eyes, and some have been found to possibly cause cancer or mess up the body's hormone and hormonal systems. Pesticides can cause neurological problems in children and other young animals, such as memory loss, coordination issues, mood swings, changes in behaviour, and problems with movement skills [69]. This is why spraying tools are crucial in addressing these issues and enhancing productivity quickly when necessary [70].

The sprinkler system has two main parts: the actual system that does the spraying and a controller. In the spraying system, you've got the stuff that's being sprayed, like pesticides or fertilizers, and a nozzle that does the spraying. The controller, on the other hand, is what triggers the nozzle to start spraying. Inside the sprinkler system, there's a pressure pump that pushes the pesticides or fertilizers through the nozzle. To control this pump and keep the pressure right, they use something called a motor driver integrated circuit. This circuit makes sure the pump gives out the right pressure as needed [71].

Spraying systems have different nozzles, each with its own way of working. They're usually found at the bottom of UAVs, and they're used to spray pesticides on crops. The system has two parts: one for controlling the spraying and the other for the nozzles. A pressure pump pushes the insecticide through the nozzle, and a special circuit helps control the pump's pressure. When it comes to utilizing spraying tools, there are two distinct methods for their use. The first kind of spraying UAV is equipped with spraying tools located on the underside of the drones [72]. The second type has the sprayer positioned under the propeller rotor. The following figures display the respective positions of the sprayer for each example [73].

2.13 QUADCOPTER MOVEMENT AND MANEUVERABILITY

Unmanned Aerial Vehicles (UAVs), specifically the Vertical Take-Off and Landing (VTOL) Quadrotors, are pilotless flying robots capable of handling missions in challenging and turbulent environments. These quadrotors have rotors positioned upwards in a square arrangement at an equal distance from the centre of the craft. Their movement is controlled by adjusting the rotational speeds of these rotors, which are powered by electric motors. Quadrotors are a common design for smaller UAVs due to their uncomplicated structure. Because of this simplicity, they find use in various tasks like surveillance, search and rescue missions, construction inspections, and more [74].

The quadrotor is a type of Vertical Take-Off and Landing (VTOL) aircraft. It's made up of four propellers arranged in either an X or + shape, with each arm carrying a rotor (made of a motor and a propeller) at its end, as depicted in the diagram. Controlling the quadrotor's movement involves adjusting the speed of the propellers, which allows it to perform various motions, including:

Roll: This movement is achieved by increasing (or decreasing) the speed of motor 1 while decreasing (or increasing) the speed of motor 3.

Pitch: It refers to the rotation around the Y axis and can be executed by increasing (or decreasing) the speed of motor 2 while decreasing (or increasing) the speed of motor 4.

Yaw: To rotate the quadrotor around the Z axis, this is accomplished by increasing or decreasing the speeds of both motors 2 and 4, or motors 1 and 3.

Forward/backward: This motion is produced by adjusting the pitch angle.

Right/left motion: It's achieved by adjusting the roll angle.

Take-off/landing: To make the quadrotor rise or descend, all motors' speeds are increased (or decreased) with the same average, resulting in an increase (or decrease) in vertical forces (thrust).

Hovering: By keeping the motors at speeds that generate thrust equal to the gravitational force, the quadrotor maintains a constant altitude and hovers in place [75].

The quadrotor is designed with its propellers and motors installed in a specific configuration: the propellers on opposing arms (1 and 3) spin in a clockwise direction (CW), while the propellers on the other set of opposing arms (2 and 4) spin in a counterclockwise direction (CCW).

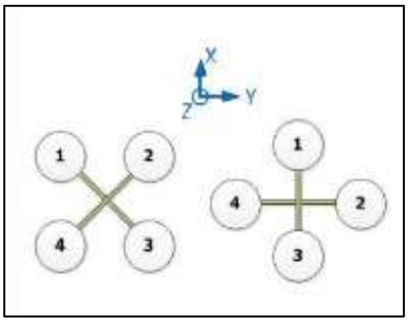

Figure 2.1: Type of drone + and ×.

2.14 ARTIFICIAL INTELLIGENCE

Artificial intelligence (AI) involves teaching machines to bring in human intelligence, enabling them to think and behave like people. This includes abilities such as learning, problem-solving, reasoning, understanding language, and perception. Essentially, AI aims to copy computers, robots, or software with intelligence like that of humans. Achieving AI involves studying human brain patterns and thinking processes. By understanding how humans think, AI researchers develop smart software and systems that can copy human-like intelligence [76]. In recent years, the use of AI in the agricultural sector has surged, driven by new innovations aimed at modernizing the industry and improving crop yields. The importance of this technology has become more pronounced, especially in response to major challenges like climate change and population growth. Traditional farming relies heavily on manual labour. Introducing AI into this process can offer several benefits. By working alongside existing technologies, smart farming systems can streamline numerous tasks. AI has the capability to gather and analyse vast amounts of data, enabling it to identify and implement optimal strategies [77]. Here are some typical examples of how AI is utilized in agriculture: enhancing automated irrigation systems, identifying leaks or damage in irrigation systems, and monitoring crops and soil conditions.

3. METHODOLOGY

3.1 DRONE FRAME AND COMPONENT DESIGNED IN SOLIDWORKS

designed for complex missions. They feature four rotors arranged in a square formation, each powered by electric motors. The quadrotor's straightforward design makes it a popular choice for small UAVs. Its performance depends on motor and propeller selection, which impact agility and payload capacity. Additionally, the frame material is critical for durability and strength, especially when carrying heavier payloads. Proper frame dimensions ensure stability and structural integrity, accommodating equipment for heavier loads. Understanding these factors aids in designing and selecting components for a drone that meets its intended tasks and payload requirements.

3.1.1 Agricultural Drone Frame

The frame of a drone is one of its most important parts; it gives the drone the stability and structure it needs to function well. This study will concentrate on the construction and composition of the type of Tarot Frame Ironman 650 drone's carbon fibre frame using the same idea. We will discuss the components of the frame and their significance in ensuring the drone's performance and durability.

The drone frame is a high-quality made of fabricated carbon, a material known for its lightweight, strong, and corrosion-resistant properties. This material makes the drone frame more durable and reduces its overall weight, allowing for longer flight times and improved stability. This frame is designed to accommodate a Tube and sprayer tube and Multispectral camera for gathering the data during the flight. The frame will be built to carry additional equipment, incorporating a crucial component for our research—an advanced sprayer capable of dispersing pesticides or water for agricultural purposes. To achieve this, we'll connect the sprayer to a land-based pump and use a tube system to transport water across substantial distances.

In the initial phase, the planning, modelling, and visual conceptualization of the agricultural drone were conducted using SolidWorks. Specifically, SolidWorks Premium 2022 was employed for these simulations. Each element comprising the quadcopter frame underwent meticulous measurement, sketching, and design within SolidWorks, ensuring precise and detailed planning of individual components.

3.1.2 Component Of the Drone

All components of the drone were exclusively drafted and designed a new within SolidWorks. Advancements in miniature sensor technology have facilitated advancements in creating smaller UAVs, such as the quadcopter [78]. Quadcopter comprises four extended arms connected to a framework that houses all the electronic components onboard. The primary section consists of the top main plate, which doubles as the bottom main plate, serving as the central housing for all electronic components. These two parts, measuring 14x15cm, play a pivotal role in accommodating the entirety of electronics.

The drone arm serves as the support structure for housing the motors, electronic speed controllers, and propellers, consisting of three integral parts. The base frame is assembled using all the components mentioned previously. The result of this assembly is illustrated. Highlighting this assembly is crucial for understanding the subsequent analysis and discussions, as it visually consolidates the integration of various elements into a cohesive system. This figure serves as a key reference point, demonstrating how each component fits together within the overall structure, thereby facilitating a deeper comprehension of the system's design and functionality.

The Frame has a 650 mm diagonal distance between the motors defines the drone's size and affects its stability, agility, and payload capacity. And can depend on the payload capacity. This measurement is crucial, as a larger diagonal implies better stability in flight and potentially allows for larger payloads or specialized equipment. Conversely, smaller diagonals often result in more agile drones suited for precise manoeuvres in confined spaces. This dimension plays a key role in determining the drone's capabilities and suitability for various tasks.

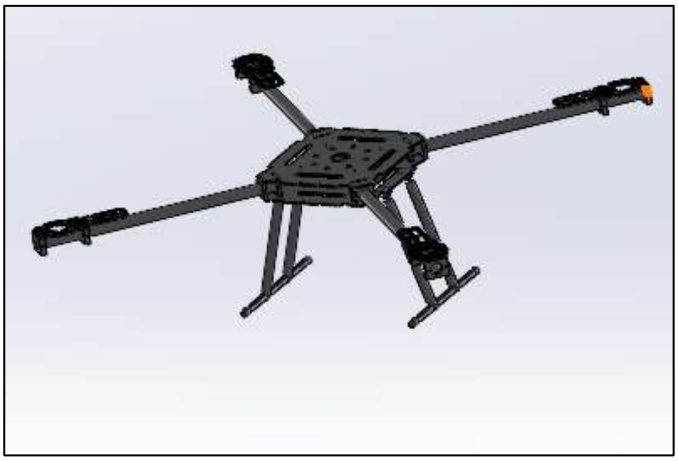

Figure 3.1: The Frame of Drone.

3.1.3 Payload Design

The payload is like a multitasking tool. It's designed to hold pipes, help with spraying, and even can carry sensors and cameras. It is a smart system that works seamlessly with the drone and spray gear, making spraying crops efficient.

Including a pipe in the drone's design brings some important benefits for spraying. First off, it makes everything much more stable. By giving a strong base for the spray gear, it stops vibrations, making sure the spraying is super accurate. Plus, this pipe helps spread out the weight of all the spraying stuff across the drone, making it easier to fly and control in the air. Having this balanced weight is a big deal for keeping the drone steady and making sure it moves exactly how we want it to during spraying.

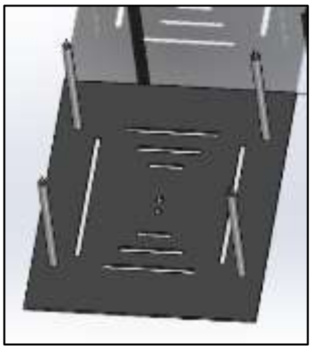

Figure 3.2: The Payload of Drone.

Figure 3.3 depicts the fully assembled main frame of a drone, which is the result of integrating all the components detailed in the previous figures. This main frame constitutes the core structure of the drone, designed to support various subsystems, including the tubing and piping necessary for its operational role in precision agriculture. Constructed from high-strength, lightweight materials, the frame is engineered to offer both durability and agility.

The central hub, which houses the drone's critical electronics such as the flight controller, navigation systems, and power units, also serves as the anchoring point for the arms that extend outward to hold the motors and rotors. These arms are key to the drone's flight capabilities, providing the necessary lift and thrust. Attached to the lower section of the frame is the specialized holder designed to carry the tubing and piping system. This part of the assembly is crucial for the drone's primary function of spraying pesticides. The design of the holder suggests a modular approach, allowing for easy attachment and removal, which facilitates maintenance and adaptability to different types of spraying tasks.

The pipes are strategically positioned to ensure optimal distribution of the spray, maximizing coverage while maintaining precision to avoid waste and minimize environmental impact. The nozzles at the tips of the pipes are likely calibrated to produce droplets of a specific size, ensuring effective application of the pesticides to the crops.

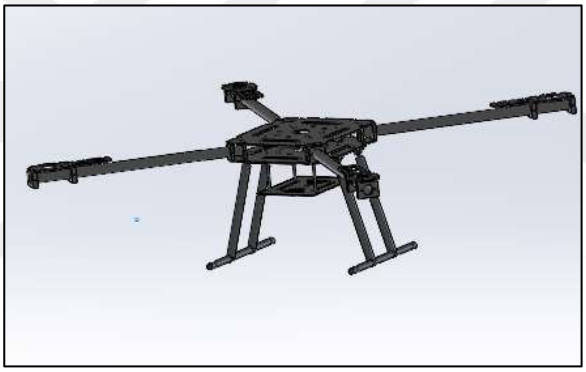

Figure 3.3: Drone Frame Assembled with Payload.

3.2 THE MATERIAL NEEDED FOR THE AGRICULTURAL DRONES

3.2.1 Drone Components

Drones rely on key components like propellers, motors, and electronic speed controllers (ESCs) to perform a variety of tasks and fly smoothly. Selecting the right combination of these components hinges upon the specific functions a drone is meant to fulfil. To determine the ideal setup, the initial step involves estimating the weight and dimensions of the payload the drone will carry. Once this payload information is known, the subsequent task involves matching the drone with the most suitable motors, propellers, and frame dimensions tailored precisely for its intended duties. A pivotal aspect governing the drone's performance is the calculation of thrust requirements. This entails ensuring that the generated thrust at maximum power (100% RPM) is at least twice the weight of the entire drone. This deliberate overestimation is essential as it empowers the drone with enhanced manoeuvrability and the capability to ascend to higher altitudes swiftly. It’s important to pick the right motors, propellers, and frame size based on what we want the drone to do and how heavy the payload is. Choosing these parts carefully ensures the drone works well and does its job effectively, no matter what it's doing or where it's flying. This way, the drone can manage different tasks smoothly and perform reliably in various situations.

3.2.2 Estimation Payload

To get a precise estimation, we first need to list all the tasks that need to be done and figure out what parts or components are necessary for each task. This process helps us understand exactly what is involved in the project and allows us to calculate the estimation accurately.

The drone is designed to spray pesticides or water for agricultural needs. One of the major challenges faced by drones is their limited flight duration due to battery capacity constraints. Additionally, their payload capacity might also be an obstacle leading to shorter operational times. The concept behind this payload aims to address these challenges. By utilizing a large tank on the ground as a base, the drone won't face limitations regarding payload capacity. This approach eliminates the need for frequent recharging as it can continuously access a full supply of water or pesticides from the base via a tube connected to a pump, ensuring uninterrupted spraying operations.

Determining the weight of the payload involves a comprehensive calculation. We consider not only the weight of the tube through which the liquid (whether it's pesticide or disinfectant) will flow, but also the weight of the pump and nozzles involved in the dispensing process. This comprehensive approach ensures an accurate assessment of the entire payload's weight, factoring in all components integral to the liquid dispersal system.

The tube weight could be found in the specification sheet that the manufacture offered for the buyer my choose is the tube high pressure that used for agricultural spraying.

Figure 3.4: Tube Chooses for Agriculture.

The tube weight it is dependent the inner diameter and outer diameter and it's given for Kg/m, the choosing tube as 12 mm as inner diameter and 15.4 mm for outer diameter the weight in kilogram for each meter depending on specific sheet it's 0.09 Kg/m then for taking 20 meters for our tasks so Total weight= 20 * 0.09= 1.8 Kilograms.

The total weight of a tube with water passing through it depends on both the inner and outer diameters of the tube. The inner diameter, which determines the space available for the water flow, and the outer diameter, which encapsulates the inner space, collectively influence the overall weight of the tube when filled with water.

Additionally, the weight of the water within the tube is directly related to its volume, which is calculated based on the cross-sectional area of the tube and the length of the water column. The density of water and the gravitational force acting on it also contribute to the overall weight of the water within the tube.

Considering these factors—inner and outer diameters, water volume, density, gravitational force, and tube material—determines the total weight of the tube when it contains water.

Inner Diameter: ID=12 mm.

As Outer Diameter: OD =15.4 mm

To calculate the volume of water passing through a tube with a length of 20 meters and an inner diameter of 12 millimetres, we first need to determine the cross-sectional area of the tube. The formula for the cross-sectional area of a hollow tube (annulus) is A and it is:

$$A = \pi \times (R_o^2 - R_i^2) \tag{3.1}$$

$$R_o = \frac{\text{Outer diameter}}{2} = \frac{15.4}{2} = 7.7 \text{ mm}$$

$$R_i = \frac{\text{inner diameter}}{2} = \frac{12}{2} = 6 \text{ mm}$$

where Ro is the outer radius and Ri is the inner radius.

Now we can find the cross-sectional area (A):

$$A = \pi \times (7.7^2 - 6^2)$$

$$=3.14 \times (59.29-36)$$

$$=73.161\ mm^2$$

The volume of water passing through the tube:

$$\text{Volume} = A \times Lengh \quad (3.2)$$

$$= 73.161 \times 20000\text{mm}$$

$$= 1{,}456{,}220 \text{ mm}^3$$

Converting the volume from cubic millimetres to Liters:

$$\text{Volume in litters} = \frac{1{,}456{,}220\ mm^3}{1{,}000{,}000} = 1.463 \text{ Liters}$$

The estimated weight of water, assuming a density of approximately 1 kg/L, would be approximately 1.463 kg for a length of 20 meters passing through the tube.

The total weight (WT) of the tube is determined based on a specified tube length of 20 meters.

WT= Weight of the tube +Weight of water

=1.463+1.8

=3.263 Kg

This calculation assumes the tube is filled with water, and the weight is an approximation based on the volume of water considering its density.

The estimated weight of the payload will rely on approximations of the component values, aiding in the determination of the overall drone weight.

3.3 THE COMPONENT OF DRONE

Successful drone flight relies on essential electronic components. The flight controller serves as the drone's brain ensuring stability and movement by processing data from sensors like gyroscopes and accelerometers. These sensors provide crucial information about the drone's orientation and speed, enabling precise control. Additionally, electronic speed controllers (ESCs) regulate the speed of the drone's motors, translating signals from the flight controller into motor outputs. Batteries power the entire system, supplying energy to the motors and electronics. GPS modules enhance navigational capabilities, enabling accurate positioning and autonomous flight. Together, these components form the foundational electronic framework necessary for safe and efficient drone operations.

In the realm of drone design, the careful selection of motors and propellers stands as a pivotal aspect, directly influencing flight performance. Motors drive propellers, determining the drone's lift capability and manoeuvrability. Matching the right motor with an appropriate propeller ensures an optimal balance between thrust and efficiency, crucial for stable flight and payload capacity.

The component selection process considers the essential elements for our drone, such as batteries, ESCs, motors, propellers, payload (tube and pump fan nozzle), connectors, and cables. The table details these components and their respective masses in grams, guiding our decision-making based on specific needs and the importance of each component in the drone's operation.

Table 3.1: Main Dimensions and Geometry Parameters of the Model.

	Components	**Mass(g)**
1	Tube + the mass of water passes through it	3263
2	Frame (body of drone)	500
3	4×Motors T-MototsM5212 420KV	1000
4	4×Propellers 15*5	164
5	Battery	max1600
6	ECS	104
7	Other components (cables-screw-.etc.)	100
8	Pump and nozzle	500
9	Total	7231-MAX 8000

Determination of the suitable motors and propellers for your drone, needs to calculate the thrust generated at 100% RPM based on the total weight carried. This calculation is crucial for selecting components that can handle your specific payload requirements and the demands of your mission. At 100% RPM, the thrust generated by the motors can typically exceed the total weight of the drone tow time at least. The adding thrust offers several advantages, notably enhancing the drone's manoeuvrability and enabling it to achieve higher altitudes at an increased rate of climb. This additional thrust-to-weight ratio ensures the drone's capability to navigate more effectively and ascend swiftly, factors crucial in optimizing its performance during various operational conditions. Based on our estimated weight, the thrust calculation will be conducted to determine the necessary propulsion force, based on the formula for how the calculate the Thrust will be suitable for better hovering.

$$\text{Thrust} = \frac{\text{The total weigh} \times 2}{\text{The numebr of rotors}} \tag{3.3}$$

To achieve the desired weight parameters, it's crucial to calculate the necessary thrust that each motor and propeller combination must generate at 100% RPM. This calculation ensures that the propulsion system can effectively support and lift the drone according to the specified weight requirements.

$$\text{Thrust} = \frac{7231 \times 2}{4}$$
$$= 3615.5\ grams$$

The total thrust generated is 14,465 grams, indicating that each motor needs to produce an additional 3615.5 grams of thrust to meet the required total thrust.

The motor selection will be determined based on the derived results indicating the required thrust specifications.

3.3.1 Motor Selection

For the motors of a drone, two primary choices exist: brushless motors and DC motors. Because of their permanent magnet rotor and advanced electronic commutation system, brushless motors have low maintenance needs, great efficiency, and less noise. They are the go-to option for drones because of their excellent efficiency and accurate control, which guarantee longer flying periods and superior overall performance [79].

However, because they depend on brushes and commutators, DC motors have a simpler design but frequently need more frequent maintenance because of brush wear. They are less desirable for drone propulsion systems even if they are appropriate for some applications because of their lower efficiency and precision when compared to brushless motors.

The motors chosen for the UAV were intended to constitute virtually the entire weight of the aircraft. These brushless motors were specifically designed to meet the additional demands for acceleration and environmental factors. Their selection was critical, as neglecting this consideration could result in difficulties controlling the UAV during take-off. Additionally, the motors were meticulously chosen not only for their ability to accommodate the weight requirements but also for their efficiency and responsiveness in adjusting to environmental influences. Their brushless design not only enhances durability but also ensures smoother and more precise operations, contributing significantly to the overall control and stability of the UAV.

According to the available data, an additional weight of 7231 units was introduced, doubling the initial weight, and resulting in a selection weight of approximately 14462 g. The table presents details about the chosen motors: specifically, the brushless DC motor identified as T-MOTOR MN5212 with a 420 KV rating. When paired with a propeller measuring 381 mm by 127 mm, each of these motors theoretically generates a lifting force of 4157 g.

Figure 3.5: T-Motor MN5212 420 KV.

Table 3.2: T-Motor MN5212 420KV Table.

Item No.	Voltage (V)	Prop	Throttle	Current (A)	Power (W)	Thrust (G)	RPM	Efficiency (G/W)	Torque (N*m)	Operating Temperature (℃)
MN5212 KV420	24	T-MOTOR 15*5CF	50%	6.8	162.2	1204	4370	7.43	0.321	53
			55%	8.7	208.1	1478	3487	7.10	0.278	
			60%	10.5	321.6	1746	5547	6.54	0.32	
			65%	12.6	302.2	1983	6376	6.36	0.374	
			75%	18.8	432.8	2589	7287	5.75	0.483	
			85%	25.0	595.9	3230	8042	5.28	0.607	
			100%	36.7	881.3	4175	8891	4.74	0.784	
		T-MOTOR 16*5.4CF	50%	8.4	202.3	1530	4615	7.56	0.301	56
			55%	10.4	250.6	1795	5210	7.16	0.354	
			60%	13.0	311.6	2165	5642	6.92	0.417	
			65%	15.7	377.3	2433	6032	6.45	0.475	
			75%	22.4	538.5	3150	6811	5.87	0.585	
			85%	29.9	715.7	3816	7485	5.33	0.743	
			100%	44.2	1061.3	4903	8435	4.63	0.963	
		T-MOTOR [illegible]	50%	10.3	235.8	1755	4686	7.16	0.376	
			55%	12.8	306.9	2071	5163	6.76	0.442	
			60%	15.9	382.2	2438	5509	6.47	0.516	

With a total of 4 of these motors on the UAV, their combined lifting capacity reaches around 16700 g. This capacity appears to be advantageous as it exceeds the total selected weight of 14462 g, ensuring a comfortable margin for transport capabilities. This table presents a detailed comparison, and specifications of motors choose, and propellers utilized 15*5 CF in drone technology, highlighting their performance characteristics and suit ability for the drone.

3.3.2 Propeller Selection

Propellers play a pivotal role in drone functionality, as they are responsible for generating lift essential for flight. Their physical characteristics such as diameter, pitch, and design directly influence how efficiently a drone can generate thrust, affecting its flight dynamics, endurance, and handling. Optimal propeller balance significantly contributes to the drone's stability and manoeuvrability. Some propeller designs prioritize minimizing noise and vibrations, leading to a smoother and more enjoyable flight experience.

Choosing a 15-inch diameter with a 5-inch pitch for the propeller involves a careful balance of factors crucial to our drone's performance. These parameters are tailored to meet specific requirements, aiming to optimize thrust generation, overall efficiency, and manoeuvring capability based on the drone's objectives.

Selecting the right propeller involves meticulous attention to the compatibility between the motor and propeller specifications. In this case, the propeller's specification sheet indicates its ability to achieve over 9000 rotations per minute (RPM) at maximum motor performance. This RPM capacity aligns precisely with the thrust requirements essential for our drone's intended application, ensuring the propeller operates within its optimal performance range.

Furthermore, our propeller's dimensions of 15 inches in diameter and 5 inches in pitch match the intended use of our drone. This choice finds a compromise between mobility, effective power usage, and the requirement for enough push. The precise pitch enhances the motor's performance and ensures the best possible balance between power consumption and lift creation, while the greater diameter helps to maximize thrust production. Taking these factors into account when choosing a propeller is essential to getting the performance and efficiency we want from our drone.

3.3.3 Electronic Speed Controllers

To manage and adapt the motor's speed according to specific requirements, we employed an electronic speed controller (ESC). Electronic speed controllers (ESCs) constitute a critical element within drones, particularly in medium- to high-range models outfitted with brushless DC motors. These ESCs play a pivotal role in governing both the speed and direction of the motors. They generally consist of several components, including a power supply stage, a current detection circuit, a microcontroller, and a communication interface linked to the flight controller. Implementation of electronic speed controller.

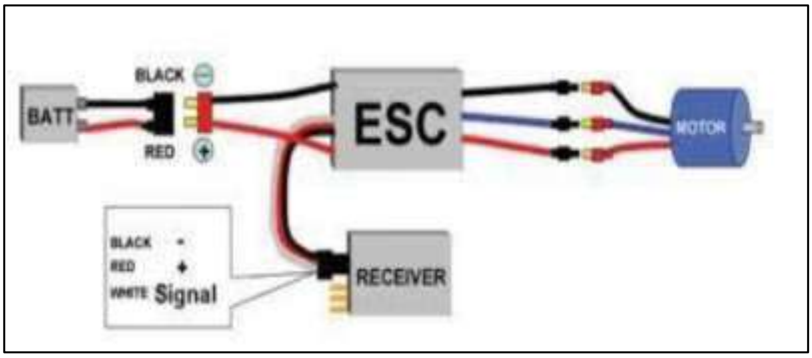

Figure 3.6: Implementation of Electronic Speed Controller.

Integrating an Electronic Speed Controller (ESC) with a brushless motor involves connecting the ESC's three output wires to the three wires of the brushless motor, ensuring a proper match of wire phases. The ESC acts as a mediator between the power source and the motor, modulating the power supply to control the motor's speed and direction. Through precise electronic commutation, the ESC determines the optimal timing and sequence to energize the motor's phases, ensuring smooth and efficient operation. This connection allows for seamless speed regulation and directional changes by adjusting the signals sent from a microcontroller or control system to the ESC. Overall, the ESC facilitates precise control and seamless integration of brushless motors into a variety of applications, such as drones, electric vehicles, and industrial machinery.

The ECS AIR 40A ESC (Electronic Speed Controller) was chosen to work in tandem with the T-Motor MN5212 due to its compatibility and appropriateness for the motor and propeller combination. The T-Motor MN5212 brushless motor and the selected propeller have certain power requirements, and the ECS air 40A ESC is designed to meet those needs. The power requirements of the motor and the ESC are in line, which guarantees optimal performance and effective power delivery to operate the propeller system and improves overall stability and performance in the intended application—likely an aerial platform or drone.

In addition to the previously mentioned components, the final assembly encompasses essential elements reflective of the actual drone setup, including components like Pixhawk and GPS. Additionally, critical to the drone's functionality is the battery, serving as the power source for components such as motors, propellers, and ECS. To ensure compatibility and optimal performance, the selected battery must operate within the voltage range of 4 to 6 cells (4-6s). Accordingly, the chosen power solution comprises a 12000mAh Lithium Polymer (LiPo) Battery, boasting a voltage rating of 22.2V. This battery configuration aligns with the operational needs of the motors, propellers, and ECS, delivering the necessary power for sustained and efficient drone operation.

The Assembly final of the spraying quadcopter drone contains all previous components mentioned Motors, propeller and electronic speed controller plus Flight controller that serves as the brains of the operation. Its primary role is to manage and control the vehicle's flight dynamics, ensuring stability, responsiveness, and control throughout the flight. Additionally, the inclusion of the "Blue tube" within this setup is critical, serving a specific purpose that justifies its placement within the overall system.

Figure 3.7: The Final Assembly of Quadcopter Drone.

Centre of mass and Moment of inertia of the drone

The calculated centre of mass for the drone, considering all integral components, provides insight into the centroid's position without considering the tubing and associated mass of water. This comprehensive analysis yields a precise understanding of the drone's balance and stability characteristics. Mass Properties of Drone.

Mass = 7231 grams

In the context of drone dynamics, particularly for a quadcopter or similar multi-rotor drone, the moments of inertia about the three principal axes (X, Y, Z) are indeed important.

The moment in kg*m² after conversion from Kg* mm²:

-$I_{xx} \approx 0.09$ kg*m²

-$I_{yy} \approx 0.09$ kg*m²

-$I_{yy} \approx 0.15$ kg*m²

3.4 MULTISPECTRAL CAMERA

For more precise agriculture, utilizing multispectral imaging is an optimal strategy for gathering data to identify the areas requiring pesticide application. Multispectral cameras are adept at capturing images of plants in both field settings and controlled environments. They operate by capturing images at distinct wavelengths spanning the electromagnetic spectrum, including near-infrared (NIR), red-edge, and visible light bands.

The drone will be outfitted with a Parrot Sequoia + multispectral camera, serving the primary purpose of vegetation characterization. This advanced camera offers a range of spectral bands, each capturing light at specific wavelengths. The variations in the number of bands, spectral range, and resolution provide a comprehensive view of the vegetation and its surrounding environment.

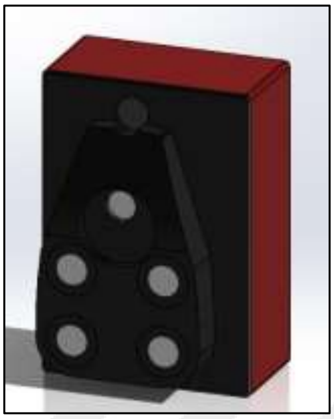

Figure 3.8: Parrot Sequoia + Design.

The Parrot Sequoia + is designed to capture multispectral imagery with high precision and accuracy. Its ability to detect light across multiple spectral bands allows for detailed analysis of vegetation health, stress levels, and growth patterns. By leveraging the unique characteristics of each band, the camera provides valuable insights into the composition and condition of the vegetation.

Our research integrates the Parrot Sequoia + multispectral camera into the drone, enhancing our understanding of vegetation and ecosystem health. This technology will help advance precision agriculture, environmental monitoring, and land management.

The drone serves as a bridge between the multispectral camera for sensing and the mechanisms for acting, facilitated by a personal computer (PC) and an RF transceiver. This setup is aimed at overcoming spraying challenges, such as cost reduction, time efficiency, and minimizing the environmental impact of chemicals. The drone collects data from the camera and transfers it to the PC for analysis to detect vegetation. The main processes involve obtaining raw data from the sensing unit, analysing the data to identify diseases and determine where to spray, and then transmitting target locations to the mechanisms for initiating spraying.

3.4.1 Data Analysis

In natural daylight, a healthy plant typically reflects only about 10% of the green colour band, with even lower reflectance in the red and blue bands due to chlorophyll absorbance. However, beyond the red edge, these plants reflect near-infrared (NIR) wavelengths close to

50%. This study employs a widely used measurement method called NDVI (Normalized Difference Vegetation Index) to assess the green density of farming fields, instead of relying on image-processing techniques in the visible spectrum. An NDVI device measures reflected light at two specific wavelengths: one close to 660 nm (in the dark red range) and another above 740 nm (in the red edge range).

NDVI, a widely recognized method in farming applications, calculates vegetation indices using electromagnetic radiation reflected from the surface of a target object. Typically, plant disease detection devices utilize two specific wavelengths: the red and near-infrared bands, to determine these indices.

The data collected and transmitted from the drone to the computer plays a pivotal role in the entire process. This data undergoes meticulous analysis to identify plant diseases and assess the overall field condition. To facilitate this analysis, various software programs and libraries for computer vision and machine learning are available. These tools aid in obtaining insightful analytics for vegetation indices.

Pix4Dfields is a specialized software designed specifically for image processing in agriculture, setting it apart from other tools. It allows users to analyse both multispectral and RGB (visible light) imagery captured by drones or other aerial platforms. With its array of features tailored for vegetation analysis, crop monitoring, and field mapping, Pix4Dfields empowers farmers and agronomists to make well-informed decisions regarding crop health, management practices, and resource allocation.

Figure 3.9: Result Analysis in Pix4Dfields.

Pix4Dfields is a unique computer program designed for farmers and field caretakers. It helps them examine pictures taken by special cameras mounted on flying machines like drones.

These images display various colours of the fields, indicating the health of plants. By using Pix4Dfields, farmers can gain deeper insights into their fields and make informed decisions about how to care for them more effectively.

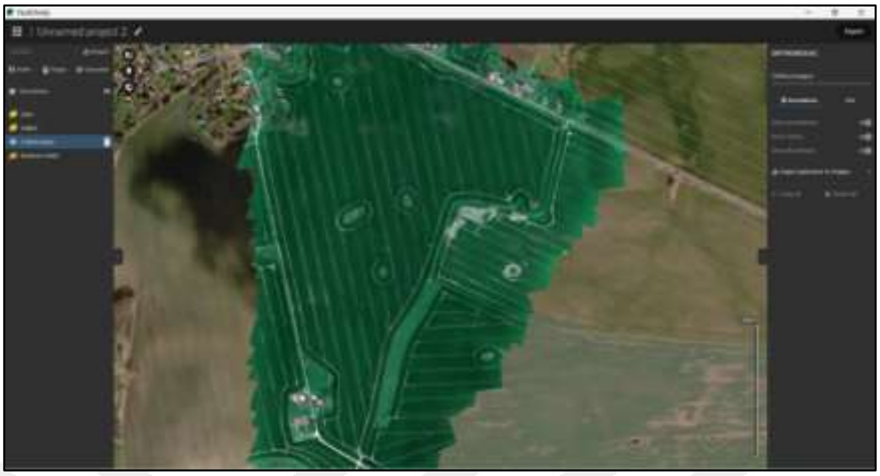

Figure 3.10: Pix4Dfield for Image Processing and Analysis.

Pix4Dfields is a software that provides a comprehensive platform for agricultural mapping, monitoring, and analysis using drone imagery. However, utilizing this software may require more knowledge to obtain precise information and may take more time to tailor solutions for various agricultural applications, such as crop health monitoring, weed detection, and yield estimation. Therefore, it is recommended to use the Agremo tool, which utilizes advanced algorithms and artificial intelligence to process multispectral and RGB imagery, providing actionable insights to farmers and agronomists. Agremo is a tool that provides farmers with more accurate solutions and a broader view of crop and vegetation health. Based on advanced algorithms and artificial intelligence, Agremo processes multispectral imagery to provide valuable statistics.

Figure 3.11: Argemo Interface Overview.

3.5 ADVANCING DRONE UTILIZATION FOR LONG-TERM YIELD OPTIMIZATION

In the pursuit of agricultural efficiency and crop management, drones have taken centre stage, offering innovative solutions for crop spraying. Yet, these advancements do not come without their own set of intricate challenges. There are two primary Obstacles that must be surmounted to harness the full potential of drone technology in agriculture: stability during the spraying process and the ability to manage substantial payloads over considerable distances. The accompanying brings these challenges into focus, showcasing a drone designed for agricultural use and hinting at the complexity of its operation. As we delve deeper into the specifics, it becomes evident that these obstacles are not merely technical but are also pivotal in determining the practicality and effectiveness of drone use in large-scale farming.

In precision farming, drones are becoming essential for tasks like spraying crops. However, keeping these drones stable while they work is a big challenge, particularly when they don't have extra support. The picture shows a drone that is made to carry up to 4 kg. But to do the job well and keep the drone easy to control, it turns out we need a motor strong enough to lift 16 kg when it's running at full power. This isn't just about carrying more weight; it's crucial for keeping up with the demands of large-scale farming. The image also shows a drone with a tube for spraying. This tube is important for spreading the spray evenly over large areas. The trouble is, the drone can get unsteady because of the forces pulling on it, making it hard to stay level in the air as shown in figure 3.12.

The challenges amplify when the drone is required to operate over extensive distances. Stability transcends being a mere operational preference to a non-negotiable necessity. The drone must not only accommodate the heft of the spraying payload but must also counteract the dynamic forces encountered during flight—forces that are intensified by the extended reach of the spraying tube. The illustration captures the drone in a moment of operation, highlighting the potential for instability due to the extended application apparatus. For drones to be viable for long-term, large-scale agricultural use, their design must prioritize a delicate equilibrium. This equilibrium involves the drone's payload capacity, energy efficiency, and the aerodynamics of sustained flight, ensuring that the drone can navigate the complexities of large field spraying while maintaining the precision and stability necessary for optimal crop yield.

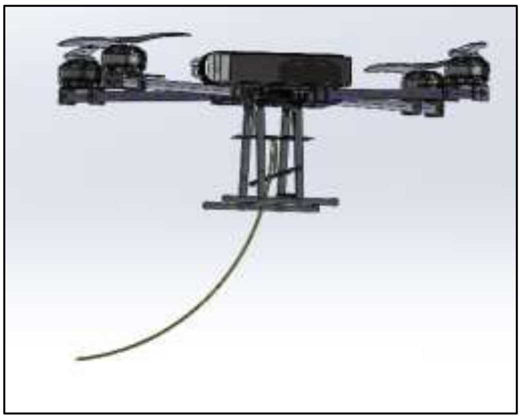

Figure 3.12: Drone Equipped with Tubing for Spraying Operations.

A novel approach to increasing precision and ensuring stability in drones used for large-area crop spraying involves the incorporation of a support system. The addition of a 2.5-meter support, as depicted in the figure, provides an innovative solution to the stability challenges previously discussed. This support system securely holds the water tube, which is a critical component of the spraying mechanism. By employing this support at intervals of every 20 meters, the drone gains enhanced steadiness during operation.

The support system functions not only as a physical stabilizer but also aids in the precise application of water or other treatment fluids over vast agricultural spaces. It enables the drone to maintain an even keel, thereby ensuring that the spray is uniformly distributed, even in windy conditions or when the drone is carrying the full capacity of its payload. This method is a leap forward in addressing the twin issues of payload management and stability, which are essential for the effective utilization of drones in modern precision agriculture.

By integrating such structural enhancements, the drones can operate over larger fields with greater efficiency and less risk of drift or operational instability. This innovation underscores the intersection of agricultural know-how and technological advancement, marking a significant stride in the evolution of farming practices.

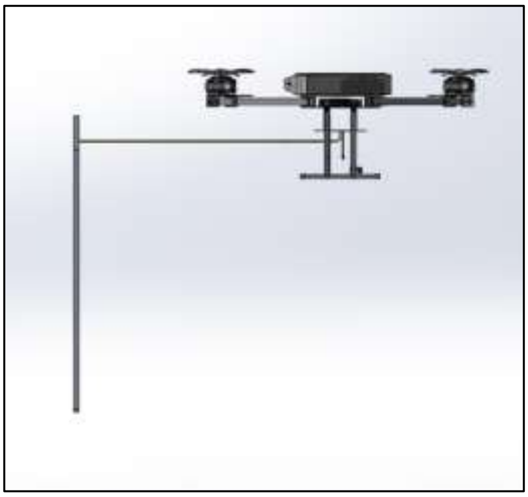

Figure 3.13: The Implementation of Support System.

3.6 MODELING, CONTROL SYSTEM DESIGN, AND SIMULINK IMPLEMENTATION: ANALYZING OUTCOMES

Quadcopters are complicated devices that function using elaborate mathematics. They are also known as four-rotor UAVs (Unmanned Aerial Vehicles). To comprehend their movement and make sure they can travel from one place to another with ease, these mathematical foundations are essential. We will explore the mathematical theories that explain the dynamics and behaviour of the quadcopter in this chapter. Additionally, we'll cover a particular kind of controller known for its proficiency in controlling the drone's orientation along the x (roll), y (pitch), and z (yaw) axes: the PID (Proportional-Integral-Derivative) controller. After laying the theoretical foundation, we will demonstrate how these ideas are really used in a Simulink design and talk about the outcomes that come from this implementation. We will gain a better understanding of the functionality and control potential of the quadcopter in real-world scenarios.

3.6.1 Mathematical Modelling

The 6 degrees of freedom model is a series of equations that captures the dynamics and whole system of the quadrotor. Every excitation or control input produces a dynamic reaction. It is possible for this dynamic response to contain one or more frequency components. We require mathematical modelling to examine that dynamic reaction. This will enable us to comprehend the dynamics of actual issues and depict the physical system in terms of governing equations. Although the non-linear equations produced by mathematical modelling will help us in controller design, this model will nonetheless be useful. These sets of equations are linearized before being used to the controller design process. Next, complicated dynamics will be controlled by the simplified dynamics controller.

3.6.2 Quadrotor Coordinate Frames

It is necessary to first present the reference coordinate systems in which the orientation, position, and transformation between these coordinate systems of the quadrotor are described as an introduction before going into detail about the mathematical model of the quadrotor. Two coordinate systems are employed for a quadrotor: the aircraft body centre frame (ABC) and the inertial (fixed) reference frame. Newton's laws hold true in an inertial frame, where the axes are oriented in the direction of North-East-Up, or ONEU. The quadrotor OABC's centre of gravity (Cog) is anchored to the body frame, which is where aerodynamic forces and torques are imparted [80].

3.6.3 Inertial Reference Frame

Earth fixed reference frame is non-accelerating, so newton's laws are valid in this frame. The origin of this reference frame serves as the starting position for the quadcopter [81].

a. The Positive x Axis is towards North.
b. The Positive y Axis is towards the East.
c. The Positive x Axis is towards the Centre of the earth.

3.6.4 Body Axis System

The body axis system is fixed with the body of the quadrotor. The centre of gravity of the quadrotor serves as the origin of the body axis system [82].

a. The Positive x Axis is towards the Forwarding direction.
b. The Positive y Axis is in the Right Direction.
c. The Positive z Axis is in a downward direction.

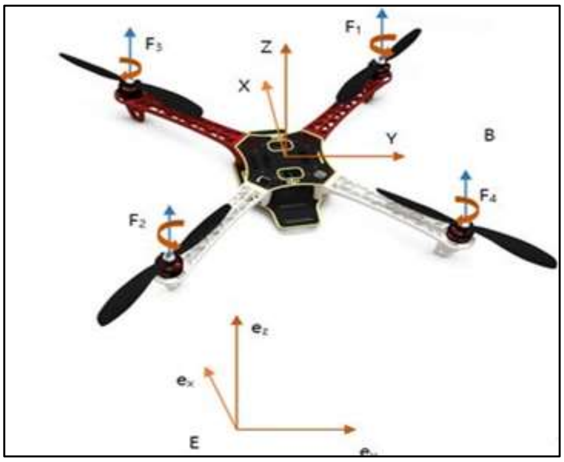

Figure 3.14: Body Axis and Inertial Axis System.

The $\{X, Y, Z\}$ denotes the body axis and $\{e_x, e_y, e_z\}$ denotes the inertial axis system. F_i denotes the forces of different motors.

3.6.5 Assumptions

To simplify our mathematical modelling and analysis, we will introduce specific assumptions to better reflect real-world conditions. In practice, certain variables have a negligible effect, and we can thus exclude these effects from our analysis. On the other hand, there are variables that introduce considerable complexity, making them difficult to address analytically. To overcome these problems, we will apply well-considered assumptions that do not significantly deviate from the reality, ensuring that our results approximate those of real-world situations closely. Despite the external mechanical simplicity of a drone, incorporating all variables into a mathematical model is a complex task. The following are the assumptions we will implement for our analysis:

a. We consider the drone as a rigid body, assuming symmetry across all axes due to its uniform structure. This assumption of rigidity is justified as the relative distances between any two points on the drone remain constant.
b. The quadrotor's propellers are likewise regarded as rigid entities since the distance between any two propellers is fixed and unchanging.
c. We will overlook complex fluid dynamic effects in our model. Accounting for these effects would complicate our ability to independently control the thrust, pitch, yaw, and roll of the quadrotor.

3.6.6 Transformation Between Reference Frames

The body-fixed frame is connected to the quadrotor's body. The frame in the body is considered an accelerating frame since it moves in conjunction with the quadrotor's motion. Newton's laws do not apply in this frame. The inertial frame is stationary relative to the centre of the earth and is considered to be a frame that does not accelerate. To apply Newton's laws, linear position and angular orientation must be converted from the body frame to the inertial frame. This translation may be achieved using methods such as Euler angles, direction cosine, and quaternions. Euler angles are straightforward to comprehend. Singularity is a condition that occurs at 90 degrees. In our situation, the Euler Angles employees follow a ZYX order of rotation.

a. 1st Rotation is about Z-axis Psi (ψ).
b. 2nd Rotation is about Y-axis Theta (θ).

c. 3rd Rotation is about X-axis Phi (φ).

Let us define the linear and angular position vectors in the inertial frame as shown in equations. The rotation matrices for each axis are written below:

$$\boldsymbol{\lambda}=\begin{bmatrix} X \\ Y \\ Z \end{bmatrix} \tag{3.4}$$

$$\boldsymbol{\eta}=\begin{bmatrix} \varphi \\ \theta \\ \psi \end{bmatrix} \tag{3.5}$$

Where **λ** represents the linear position in the inertial frame and η represents the angular position in terms of the Euler angles (ϕ, θ, ψ) in the inertial frame. Euler angles are three angles that represent the orientation of a vector in three-dimensional space [83].

In the study of quadrotor dynamics, rotating the body frame along its three principal axes-typically referred to as roll, pitch, and yaw-is essential for orientation control. This rotation process allows the definition of linear and angular velocities in the inertial frame, crucial for flight navigation and control. The linear and angular velocities are represented by vectors in the inertial frame, enabling the application of Newton's laws for motion prediction and control system design in quadrotors.

$$V_I=\begin{bmatrix} \dot{x} \\ \dot{y} \\ \dot{z} \end{bmatrix} \tag{3.6}$$

$$\omega_E=\begin{bmatrix} \dot{\varphi} \\ \dot{\theta} \\ \dot{\psi} \end{bmatrix} \tag{3.7}$$

Where V_I represents the linear velocities and ω_E represents the Euler angle rates in the inertial frame. Now let us define the velocity vectors in the body frame.

$$V_B=\begin{bmatrix} u \\ v \\ w \end{bmatrix} \tag{3.8}$$

$$\omega_B=\begin{bmatrix} p \\ q \\ r \end{bmatrix} \tag{3.9}$$

Where V_B is the linear and ω_B is the angular velocity vector in the body frame. At this point, every position and velocity vector required for the inertial and body frames has been specified. The next sections will comprise the definition of matrices that establish relationships between vectors in distinct frames.

To rotate a vector in three-dimensional space, it indeed needs to be multiplied by a rotation matrix. This matrix is constructed based on the angle and axis of rotation, following specific mathematical rules [84].

The rotation matrix for rotation about Z-Axis is,

$$R_z(\psi) = \begin{bmatrix} \cos\psi & \sin\psi & 0 \\ -\sin\psi & \cos\psi & 0 \\ 0 & 0 & 1 \end{bmatrix} \tag{3.10}$$

The rotation matrix for rotation about Y-Axis is,

$$R_y(\theta) = \begin{bmatrix} \cos\theta & 0 & -\sin\theta \\ 0 & 1 & 0 \\ \sin\theta & 0 & \cos\theta \end{bmatrix} \tag{3.11}$$

The rotation matrix for rotation about X-Axis is,

$$R_x(\varphi) = \begin{bmatrix} 1 & 0 & 0 \\ 0 & \cos\varphi & \sin\varphi \\ 0 & -\sin\varphi & \cos\varphi \end{bmatrix} \tag{3.12}$$

Hence, the transformation from Inertial to body and body to inertial frame becomes (T),

$$T_I^B = R(\varphi)R(\theta)R(\psi) \tag{3.13}$$

$$T_I^B = \begin{bmatrix} 1 & 0 & 0 \\ 0 & \cos\varphi & \sin\varphi \\ 0 & -\sin\varphi & \cos\varphi \end{bmatrix} \begin{bmatrix} \cos\theta & 0 & -\sin\theta \\ 0 & 1 & 0 \\ \sin\theta & 0 & \cos\theta \end{bmatrix} \begin{bmatrix} \cos\psi & \sin\psi & 0 \\ -\sin\psi & \cos\psi & 0 \\ 0 & 0 & 1 \end{bmatrix} \tag{3.14}$$

$$\mathrm{T_I^B} = \begin{bmatrix} \cos\theta\cos\psi & -\cos\theta\sin\psi & -\sin\theta \\ \sin\theta\sin\varphi\cos\psi + \sin\psi\cos\phi & \sin\psi\sin\theta\sin\varphi + \cos\psi\cos\varphi & \sin\varphi c\theta \\ \sin\theta\cos\varphi\cos\psi + \sin\psi\sin\phi & \sin\psi\sin\theta\cos\varphi - \cos\psi\sin\varphi & \cos\varphi\cos\theta \end{bmatrix} \tag{3.15}$$

Since the three matrices above are orthogonal, the resulting rotation matrix is likewise orthogonal. According to this fact, we understand that given an orthonormal matrix, the inverse of the matrix is equal to its transpose [85].

$$[T_I^B]^T = T_B^I \tag{3.16}$$

$$T_B^I = [T_I^B]^{-1}$$

$$[T_I^B]^T = [R_I^B]^{-1}$$

$$T_B^I = \begin{bmatrix} cos\psi cos\theta & sin\theta cos\psi sin\varphi - sin\psi cos\varphi & cos\theta sin\psi cos\varphi - sin\psi sin\varphi \\ sin\psi cos\theta & sin\theta sin\psi sin\varphi + cos\psi cos\varphi & sin\theta sin\psi cos\varphi - cos\psi sin\varphi \\ -sin\theta & cos\theta sin\varphi & cos\theta sin\varphi \end{bmatrix} \tag{3.17}$$

T_B^I,The transformation from body to inertial frame becomes.

3.6.7 Kinematics

Kinematics is a branch of mechanics that deals with the movement of objects in a robotic system without considering the forces or torques responsible for the movement. Robot design, analysis, control, and simulation are fundamentally based on kinematics due to the nature of robotic systems being intended for motion. The robotics community has concentrated on effectively utilizing various forms of position and orientation representations and their time derivatives to address fundamental kinematics issues [86].

In the context of quadrotor dynamics, kinematics is crucial for describing the translational and rotational motions of the vehicle. This involves using linear position vectors and Euler angles or quaternions to express the quadrotor's orientation and position in space. These kinematic descriptions enable the translation of motion from the body-fixed frame to the inertial frame, essential for accurately applying Newton's laws and controlling the quadrotor's flight path.

3.6.8 Translation Motion

The transformation matrix is a crucial kinematics tool for converting quadrotor position and velocities from the body frame to the earth frame, enabling accurate description of the vehicle's motion and enabling effective navigation and control strategies, the equations can be expressed as:

$$\begin{bmatrix} \dot{x} \\ \dot{y} \\ \dot{z} \end{bmatrix} = [T_B^I] \begin{bmatrix} u \\ v \\ w \end{bmatrix} \tag{3.18}$$

$$\begin{bmatrix} \dot{x} \\ \dot{y} \\ \dot{z} \end{bmatrix} = \begin{bmatrix} \boldsymbol{cos\psi cos\theta} & \boldsymbol{sin\theta cos\psi sin\varphi - sin\psi cos\varphi} & \boldsymbol{cos\theta sin\psi cos\varphi - sin\psi sin\varphi} \\ \boldsymbol{sin\psi cos\theta} & \boldsymbol{sin\theta sin\psi sin\varphi + cos\psi cos\varphi} & \boldsymbol{sin\theta sin\psi cos\varphi - cos\psi sin\varphi} \\ \boldsymbol{-sin\theta} & \boldsymbol{cos\theta sin\varphi} & \boldsymbol{cos\theta sin\varphi} \end{bmatrix} \begin{bmatrix} \boldsymbol{u} \\ \boldsymbol{v} \\ \boldsymbol{w} \end{bmatrix} \tag{3.19}$$

The linear velocity equations in the inertial frame are:

$$\dot{x} = (\cos\psi\cos\theta)u + (\sin\theta\cos\psi s\varphi - \sin\psi\cos\varphi) + (\cos\theta\sin\psi c\varphi - \sin\psi\sin\varphi)w.$$

$$\dot{y} = (\sin\psi\cos\theta)u + (\sin\theta\sin\psi\sin\varphi + \cos\psi\cos\varphi)v + (\sin\theta\sin\psi\cos\varphi - \cos\psi\sin\varphi)w.$$

$$\dot{z} = -(\sin\theta)u + (\cos\theta\sin\varphi)v + (\cos\theta\sin\varphi)w$$

The T_I^B matrix is instrumental in analyzing how earth-related forces, such as gravity, affect the body frame, while the T_B^I matrix facilitates the representation of forces and linear velocities existing on the body frame within the inertial frame. This establishes a connection between the linear velocities across both reference frames, which can be illustrated as follows:

$$V_I = T_B^I \, V_B \tag{3.20}$$

$$V_B = T_I^B \, V_I \tag{3.21}$$

3.6.9 Angular Velocity Transformation

To maintain continuity between the Body and Earth frames, a transformation matrix links vehicle angular velocities with Euler angles' time derivatives, enabling navigation and control calculations. Equation 3.22 explains this relationship, though specific formulations provide more details:

$$\omega_B = \mathrm{T_I^B} \times \omega_E \tag{3.22}$$

$$\begin{bmatrix} p \\ q \\ r \end{bmatrix} = \begin{bmatrix} 1 & 0 & -sin\theta \\ 0 & cos\psi & sin\psi cos\theta \\ 0 & -sin\psi & cos\psi cos\theta \end{bmatrix} \times \begin{bmatrix} \dot{\varphi} \\ \dot{\theta} \\ \dot{\psi} \end{bmatrix}$$

The matrix referred to as $\mathbf{T_E^B}$ is the angular velocity transformation matrix. It converts the rates of change of Euler angles into body angular velocities. This pivotal matrix helps understand how changes in the vehicle's orientation, described by Euler angles, translate into angular velocities in the body frame, enabling precise control and navigation.

$$\mathbf{T_I^B} = \begin{bmatrix} \mathbf{1} & \mathbf{0} & -\boldsymbol{sin\theta} \\ \mathbf{0} & \boldsymbol{cos\psi} & \boldsymbol{sin\psi cos\theta} \\ \mathbf{0} & -\boldsymbol{sin\psi} & \boldsymbol{cos\psi cos\theta} \end{bmatrix} \tag{3.23}$$

The transformation of the angular velocities from the body frame to the Euler rates could also be achieved the same way as in the previous section by the inverse of the **TIB** matrix.

$$\mathbf{T_I^B} = \mathbf{T_B^I}^{-1} \tag{3.24}$$

The $\mathrm{T_B^E}$ matrix is given as in the equation:

$$\mathrm{T_B^I}^{-1} = \begin{bmatrix} 1 & \sin\varphi\tan\theta & -\cos\varphi\tan\theta \\ 0 & \cos\varphi & -\sin\varphi \\ 0 & \sin\varphi/\cos\theta & \cos\varphi/\cos\theta \end{bmatrix} \tag{3.25}$$

The T_B^I matrix invers can be used to represent the angular velocities obtained from the sensors on the quadrotor, as the Euler angle rates in the inertial frame. Likewise, the $\mathrm{T_I^B}$ matrix can be used to transfer the angular velocities that exist on earth, to the body frame. Finally, the relation between the angular velocities can be shown as:

$$\boldsymbol{\omega_E} = \mathbf{T_B^{I}}^{-1} \times \boldsymbol{\omega_B} \quad (3.26)$$

$$\boldsymbol{\omega_B} = \mathbf{T_I^{B}} \times \boldsymbol{\omega_E} \quad (3.27)$$

With the definition of all rotation and transformation matrices which show the linear and angular relations, The set of angular equations of motion in the inertial frame can be written as

$$\begin{bmatrix} \dot{\varphi} \\ \dot{\theta} \\ \dot{\psi} \end{bmatrix} = \begin{bmatrix} p + q(sin\varphi tan\theta) + r(cos\varphi tan\theta) \\ q(cos\varphi - r \times sin\varphi) \\ q(sin\varphi/cos\theta + r * cos\varphi/cos\theta \end{bmatrix}$$

3.6.10 Dynamic Model of The Quadrotor

Dynamics in the context of a quadrotor refers to studying how forces and torques, generated primarily by the spinning rotor propellers to produce thrust, influence the vehicle's motion. Utilizing Newton's second law, these forces and moments are calculated within an inertial frame to understand and predict the quadrotor's behaviour under various conditions, enabling precise control over its flight [87].

3.6.11 Newton – Euler Equations

The current study utilizes the Newton-Euler representations of dynamical equations, as they are extensively documented in the literature concerning quadrotor analysis. In the inertial frame, the most comprehensive form of these equations is depicted. Additional correction terms need to be included when presenting these equations in the body frame. The Newton-Euler equations are mathematically represented in the body frame as follows [88].

$$\mathrm{m}\dot{V}_B + \mathrm{m}\omega_B \times V_B = \sum \mathrm{F_B} \quad (3.28)$$

$$\mathrm{I}\dot{\omega}_B + \omega_B \times I\ \omega_B == \sum \mathrm{M_B} \quad (3.29)$$

M : The mass of rigid body.

I : The inertia matrix.

$\sum F_B$: The external Forces.

$\sum M_B$: The external moments.

The inertia matrix and external forces and moments acting on the rigid body represented in the body frame. We can see in the equation 3.30 and 3.31 the elements matrix of inertia and external forces and moments.

$$\sum F_B = \begin{bmatrix} F_x \\ F_y \\ F_z \end{bmatrix} \quad (3.30)$$

$$\sum M_B = \begin{bmatrix} M_x \\ M_y \\ M_z \end{bmatrix} \quad (3.31)$$

$$I = \begin{bmatrix} I_{xx} & I_{xy} & I_{xz} \\ I_{yx} & I_{yy} & I_{yz} \\ I_{zx} & I_{zy} & I_{zz} \end{bmatrix} \quad (3.32)$$

Considering the assumptions we have established; the matrix can be represented as:

$$I = \begin{bmatrix} I_{xx} & 0 & 0 \\ 0 & I_{yy} & 0 \\ 0 & 0 & I_{zz} \end{bmatrix} \quad (3.33)$$

3.6.11.1 Forces equations

The forces are described with the help of the equations below.

$$F = \frac{d}{dt}(mV)_E \quad (3.34)$$

$$\begin{bmatrix} F_x \\ F_y \\ F_z \end{bmatrix} = m \times \begin{bmatrix} \dot{u} \\ \dot{v} \\ \dot{w} \end{bmatrix} + \begin{bmatrix} p \\ q \\ r \end{bmatrix} \times m \begin{bmatrix} u \\ v \\ w \end{bmatrix} \quad (3.35)$$

After the mathematical expression, the result for the matrix of forces is presented, as indicated by the equations.

$$\begin{bmatrix} F_x \\ F_y \\ F_z \end{bmatrix} = \begin{bmatrix} m(\dot{u} + wq - rv) \\ m(\dot{v} + ru - pw) \\ m(\dot{w} + pv - qu) \end{bmatrix} \quad (3.36)$$

To express the linear motion equations in terms of the linear accelerations in the body frame, one can rearrange the dynamical equations that describe the motion of a rigid body. By focusing on the accelerations $\dot{u}, \dot{v}, \dot{w}$ and along the body's x, y, and z axes respectively, and how they relate to the forces F_x F_y and F_z a more direct representation of the body's acceleration due to these forces can be achieved. which represents the forces acting on the body as the formula.

can be reformulated to focus on acceleration, resulting in Equation 3.37:

$$\begin{bmatrix} \dot{u} \\ \dot{v} \\ \dot{w} \end{bmatrix} = \begin{bmatrix} \frac{F_x}{m} + rv - qw \\ \frac{F_y}{m} + (pw - ru) \\ \frac{F_z}{m} + (qu - pu) \end{bmatrix} \quad (3.37)$$

This reformulation provides a clear view of how the accelerations in the body frame $(\dot{u}, \dot{v}, \dot{w})$ are influenced not only by the applied forces (F_x, F_y, F_z) normalized by the mass m, but also by the interplay of rotational velocities (p, q, r) and linear velocities (u, v, w). This perspective is particularly useful in the design and analysis of control systems for rigid bodies, such as quadrotors and other flying vehicles, where understanding the relationship between forces, accelerations, and the body's orientation and velocity is crucial for stability and manoeuvrability.

3.6.11.2 Moment equations

The equations of moments are derived by taking the mathematical derivative of angular momentum, a key concept in classical mechanics. These equations are crucial in understanding and analysing the dynamics of rotating systems, as they describe how the moment affects an object's rotational motion. The resulting equation is a cornerstone in rotational dynamics study.

$$\begin{bmatrix} M_x \\ M_y \\ M_z \end{bmatrix} = \begin{bmatrix} I_{xx} & 0 & 0 \\ 0 & I_{yy} & 0 \\ 0 & 0 & I_{zz} \end{bmatrix} \begin{bmatrix} \dot{p} \\ \dot{q} \\ \dot{r} \end{bmatrix} + \begin{bmatrix} p \\ q \\ r \end{bmatrix} \begin{bmatrix} I_{xx} & 0 & 0 \\ 0 & I_{yy} & 0 \\ 0 & 0 & I_{zz} \end{bmatrix} \begin{bmatrix} u \\ v \\ w \end{bmatrix} \quad (3.38)$$

Considering the assumptions we have established; the result can be represented as:

$$\begin{bmatrix} M_x \\ M_y \\ M_z \end{bmatrix} = \begin{bmatrix} L \\ M \\ N \end{bmatrix} = \begin{bmatrix} I_{xx}\dot{p} + \left(I_{zz} - I_{yy}\right)qr \\ I_{yy}\dot{q} + (I_{xx} - I_{zz})rp \\ I_{ZZ}\dot{r} + \left(I_{yy} - I_{xx}\right)pq \end{bmatrix} \quad (3.39)$$

To express the equations with a focus on angular accelerations, it is essential to isolate the angular accelerations on the left side of the equation. This approach yields the equations, as illustrated in the equations provided below.

$$\dot{p} = \frac{1}{I_{xx}}[(I_{yy} - I_{zz})qr + M_x] \quad (3.40)$$

$$\dot{q} = \frac{1}{I_{yy}}[(I_{zz} - I_{xx})rp + M_y] \quad (3.41)$$

$$\dot{r} = \frac{1}{I_{zz}}[(I_{xx} - I_{yy})qp + M_z] \quad (3.42)$$

3.6.11.3 External forces

Various external forces impact the flight dynamics of a quadrotor. The collective effect of these forces determines the overall net force exerted on the quadrotor. Equation 3.41 below outlines the components that make up the total external forces acting on the quadrotor.

$$\sum F_B = F_M + F_G + F_w \quad (3.43)$$

Where F_M represents the force generated by the motors, F_G is the gravitational force acting upon the quadrotor, and F_w denotes the force exerted by the wind.

The forces produced by the motors specifically influence the ZB axis within the body frame. As mentioned earlier, the motors can generate forces exclusively in the negative Z direction. This limitation arises from the aerodynamic design of the propellers, which are constructed to exert substantial force only in one direction. Given that the motors exert no influence over the other two primary axes of the body frame, the motor-generated forces are represented as in the matrix below:

$$F_M = \begin{bmatrix} 0 \\ 0 \\ f_m \end{bmatrix} \tag{3.44}$$

Where the f_m is the sum of generated by the four motors:

$$f_m = f_{m1} + f_{m2} + f_{m3} + f_{m4} \tag{3.45}$$

Gravity represents another pivotal source of external force, consistently directed towards the Earth's centre, a direction previously established as +zi within the inertial frame. To accurately account for external forces within the body frame of reference, it's essential to translate the gravitational force from the inertial frame. This translation is straight forwardly accomplished through the application of the rotation matrix R_I^B, which has been previously defined. Consequently, the representation of gravitational force within the body frame can be articulated as per equation 3.46.

$$F_G = T_I^B \begin{bmatrix} 0 \\ 0 \\ mg \end{bmatrix} \tag{3.46}$$

Lastly the external force affecting the quadrotor comes from wind F_w, which can exert its influence across all three principal axes of the body frame. This wind force is variable and can be represented as follows:

$$F_w = \begin{bmatrix} f_{wx} \\ f_{wy} \\ f_{wz} \end{bmatrix} \tag{3.47}$$

Finally, the equation for the external force is presented as shown in equation 3.43, before detailing each type of external force impacting the drone:

$$\sum F_B = \begin{bmatrix} 0 \\ 0 \\ f_m \end{bmatrix} + T_I^B \begin{bmatrix} 0 \\ 0 \\ mg \end{bmatrix} + \begin{bmatrix} f_{wx} \\ f_{wy} \\ f_{wz} \end{bmatrix} \tag{3.48}$$

It's important to recognize that accurately predicting or measuring the wind force impacting the quadrotor is a complex challenge, which consequently complicates the dynamic model of the aircraft. Considering that this study focuses on a nano-quadrotor, which is predominantly intended for indoor use, it is reasonable for the sake of simplification to assume the absence of wind forces acting on the quadrotor in our scenario.

Therefore, by eliminating the wind force from our considerations and applying the rotation matrix to the gravity vector, we can derive a simplified expression for the external forces. This streamlined formula is explicitly presented in the following equation:

$$\begin{bmatrix} F_x \\ F_y \\ F_z \end{bmatrix} = \begin{bmatrix} -mg(Sin\theta) \\ mg(sin\varphi cos\theta) \\ m(cos\varphi cos\theta) - f_m \end{bmatrix} \tag{3.49}$$

3.6.11.4 External moments

Similar to external forces, various sources of external moments also exist, with their sum constituting the total external moments acting on the body frame. The composition of these total external moments is outlined in the equation below.

$$\sum M_B = M_M + M_G + M_w \tag{3.50}$$

With M_M denotes the moments produced by the motors, M_G represents the gyroscopic moments affecting the quadrotor, and M_w refers to the moments generated by the wind. Each motor within the quadrotor system is designed to generate a moment in a specific direction, either clockwise (CW) or counterclockwise (CCW), along the **Z_B** axis of the body frame. While a motor's torque is confined to a single axis, the forces it exerts can induce torques across the other principal axes of the body frame, as explained in section before. Consequently, the torques generated by the motors are defined in vector form, as presented in equation below.

$$M_M = \begin{bmatrix} m_{mx} \\ m_{my} \\ m_{mz} \end{bmatrix} \tag{3.51}$$

Gyroscopic moments are caused by an object's tendency to maintain its angular momentum. When rotating along an axis, a torque applied to another axis creates a torque in a third axis, creating a gyroscopic effect. This phenomenon is present in quadrotor systems, as shown in equation below.

$$M_G = \omega_B \begin{bmatrix} 0 \\ 0 \\ j\Omega_G \end{bmatrix} \tag{3.52}$$

Where j is the inertia of the motors and Ω_G is the sum of propeller speed:

$$\boldsymbol{\Omega_G = -\Omega_1 + \Omega_2 - \Omega_3 + \Omega_4} \quad (3.53)$$

The final source of external moment to account for is the moments induced by the wind. Given the wind's capability to flow in any direction, it has the potential to generate torques along all three axes of the body frame. Therefore, the vector representing the moments attributed to wind forces is depicted as follows.

$$\mathrm{M_w} = \begin{bmatrix} \mathrm{m_{wx}} \\ \mathrm{m_{wy}} \\ \mathrm{m_{wz}} \end{bmatrix} \quad (3.54)$$

The total external moments acting on the quadrotor $\sum \mathrm{M_B}$ can be shown as in equation below:

$$\sum \mathrm{M_B} = \begin{bmatrix} m_{mx} \\ m_{my} \\ m_{mz} \end{bmatrix} + \omega_B \begin{bmatrix} 0 \\ 0 \\ j\Omega_G \end{bmatrix} + \begin{bmatrix} m_{wx} \\ m_{wy} \\ m_{wz} \end{bmatrix} \quad (3.55)$$

Given the assumption of operating within an indoor environment, as outlined in the previous section, we can disregard the moments produced by wind. This allows for a simplified representation of the total external moments acting on the body frame. Consequently, this simplified form of total external moments is explicitly presented in equation 3.56.

$$\sum \mathrm{M_B} = \begin{bmatrix} \mathrm{m_x} \\ \mathrm{m_y} \\ \mathrm{m_z} \end{bmatrix} = \begin{bmatrix} \mathrm{m_{mx}} + \mathrm{qj}\Omega_\mathrm{G} \\ \mathrm{m_{my}} - \mathrm{pj}\Omega_\mathrm{G} \\ \mathrm{m_{mz}} \end{bmatrix} \quad (3.56)$$

3.6.12 Input Dynamics

The study identifies four key inputs for quadrotor control: 'Thrust', 'Roll Torque', 'Pitch Torque', and 'Yaw Torque'. These inputs are crucial for altitude, orientation, and position adjustments, enabling desired flight dynamics.

The input vector contains the inputs to the quadrotor given by:

$$U = [U_1\ U_2\ U_3\ U_4]^T \quad (3.57)$$

$$U_1 = b(\Omega_1^2 + \Omega_2^2 + \Omega_3^2 + \Omega_4^2) \quad (3.58)$$

$$U_2 = bl(-\Omega_2^2 + \Omega_4^2) \quad (3.59)$$

$$U_3 = bl(-\Omega_1^2 + \Omega_3^2) \quad (3.60)$$

$$U_4 = d(-\Omega_1^2 + \Omega_2^2 - \Omega_3^2 + \Omega_4^2) \quad (3.61)$$

Where Ω1, Ω2, Ω3 and Ω4 are the propeller speeds that are based on the configuration chosen which is specified in section.

In the above equation the first input U_1 consists of the total thrust of all the four actuators, while U_2 is the pitch moment, U_3 represents the roll moment and U_4 represents the yaw moment. b represents the thrust factor; d represents the drag factor and l represents the length of the moment arm. The above set of equations is also known as the motor mixing algorithm.

In our specific scenario, it is crucial to note that we do not require the direct calculation of these input vectors since we have access to detailed motor specifications provided in the motor datasheets. These specifications offer precise values for the thrust, pitch, roll, and yaw moments based on the motor's performance characteristics. As such, the necessity to manually compute these inputs through the motor mixing algorithm is bypassed, allowing for a more streamlined integration and implementation of the motor's operational parameters into the quadrotor's control system. This approach significantly simplifies the design and optimization process, ensuring that the quadrotor's performance closely aligns with the expected outcomes based on the motor manufacturer's specifications.

3.6.13 State Equations

State-space representation serves as a highly effective method for depicting dynamical systems. As these systems increase in complexity, the traditional transfer function approach struggles to accurately represent them. In contrast, the state-space model facilitates the observation and control of specific system states concurrently. This feature makes it especially suited for managing multiple input-multiple output (MIMO) systems, providing a more practical framework for handling such systems. Essentially, the state-space representation is composed of two primary equations [89].

$$\dot{x} = Ax + Bu \tag{3.62}$$

$$y = Cx + Du \tag{3.63}$$

where:

u: Control input vector

x: State Victor.

y: Output Victor.

A: System matrix

B : Input matrix.

C : Output matrix.

D: Feedforward matrix.

Typically, a quadcopter system encompasses twelve state variables and four control inputs. both the state variables and the control inputs can be described using the following representation:
The state variables are commonly chosen to include both linear and angular positions and velocities within the inertial frame, as these are directly related to the Earth. Meanwhile, the control input variables are determined based on the forces and moments produced by the motors, over which we have direct control. Consequently, the state and control input vectors, incorporating these actual variables, can be outlined as follows:
x vector can be written as:

$$x = \left[\, \dot{x}\; \dot{y}\; \dot{z}\; \ddot{x}\; \ddot{y}\; \ddot{z}\; \dot{\psi}\; \dot{\theta}\; \dot{\varphi}\; \dot{p}\; \dot{q}\; \dot{r} \right]^T \tag{3.64}$$

u : Input vector:

$$u=\begin{bmatrix} U_1 \\ U_2 \\ U_3 \\ U_4 \end{bmatrix} \tag{3.65}$$

From equation 3.62, It becomes necessary to define the derivatives of all state variables. Thus, we need to specify the $\dot{V}_I$ and $\dot{\omega_E}$ vectors, which include the derivatives of the linear and angular velocities, respectively.
Newton's equation of motion, initially formulated in the body frame as presented in equation 3.26, can be transposed to the inertial frame in the following manner.

$$m\dot{V}_I=\sum F_I \tag{3.66}$$

Will be converted from the body frame to the inertial frame by using the transformation matrix T_I^B

$$m\dot{V}_I=T_B^I\sum F_I$$

$$=T_B^I F_M + T_B^I F_G$$

From equations 3.42 and 3.43, we can continue in terms of the control input vector.

$$m\dot{V}_I=T_B^I\begin{bmatrix} 0 \\ 0 \\ -U_1 \end{bmatrix}+T_B^I T_I^B\begin{bmatrix} 0 \\ 0 \\ mg \end{bmatrix} \tag{3.67}$$

$$T_B^I \times T_I^B=1 \tag{3.68}$$

$$=T_B^I\begin{bmatrix}0\\0\\-U_1\end{bmatrix}+\begin{bmatrix}0\\0\\mg\end{bmatrix}$$

Dividing both sides with m yields:

$$\dot{V}_I = T_B^I\begin{bmatrix}0\\0\\\frac{-U_1}{m}\end{bmatrix}+\begin{bmatrix}0\\0\\g\end{bmatrix} \quad (3.69)$$

By doing the calculation we can finally write the in explicit form as in equation:

$$\dot{V}_I = \begin{bmatrix}\ddot{x}\\\ddot{y}\\\ddot{z}\end{bmatrix}=\begin{bmatrix}\frac{-U_1}{m}(\cos\varphi\sin\theta\cos\psi+\sin\varphi\sin\psi)\\\frac{-U_1}{m}(\cos\varphi\sin\theta\sin\psi-\sin\varphi\cos\psi)\\g-\frac{U_1}{m}(\cos\varphi\cos\theta)\end{bmatrix} \quad (3.70)$$

To define, additional assumptions can be made regarding the quadrotor's manoeuvring capabilities. Specifically, it is not necessary for the quadrotor to undergo significant tilting to move left-right or forward-backward while airborne. Consequently, we can assume that the two tilt angles, φ and θ, are approximately zero. This assumption simplifies the T_B^I matrix presented in equation 3.17 to an identity matrix, thereby establishing a direct relationship between the body's angular rates and Euler rates as follows:

$$\omega_E = I_{3*3}\omega_B \quad (3.71)$$

$$\omega_B=\omega_E \quad (3.72)$$

Taking the derivative of both sides' yields:

$$\dot{\omega}_E = \dot{\omega}_B \quad (3.73)$$

$$\begin{bmatrix}\ddot{\varphi}\\\ddot{\theta}\\\ddot{\psi}\end{bmatrix}=\begin{bmatrix}\dot{p}\\\dot{q}\\\dot{r}\end{bmatrix} \quad (3.74)$$

Through the process of substituting equations 3.74 into equation 3.40, 3.41and 3.42, and by referring to the notations for the control input vector as defined in equation previously , we can construct the final form of the derivative of the Euler rates vector, $\dot{\omega}_E$.

$$\begin{bmatrix}\ddot{\varphi}\\\ddot{\theta}\\\ddot{\psi}\end{bmatrix}=\begin{bmatrix}\frac{1}{I_{xx}}[(I_{xx}-I_{zz})qr+M_x]\\\frac{1}{I_{yy}}[(I_{zz}-I_{xx})rp+M_y]\\\frac{1}{I_{zz}}[(I_{xx}-I_{yy})qp+M_z]\end{bmatrix} \quad (3.75)$$

The following represents the comprehensive set of equations derived from the dynamic and kinematic modelling of the quadrotor within a 6DOF (six degrees of freedom) environment. These equations encompass the twelve state variables as determined through the application of the state-space equations 3.76, with the outcomes illustrated below:

$$\dot{x} = (c\psi c\theta)u + (s\theta c\psi s\varphi - s\psi c\varphi)v + (c\theta s\psi c\varphi - s\psi s\varphi)w \tag{3.76}$$

$$\dot{y} = (c\theta)u + (s\theta s\psi s\varphi + c\psi c\varphi)v + (s\theta s\psi c\varphi - c\psi s\varphi)w \tag{3.77}$$

$$\dot{z} = -(s\theta)u + (c\theta s\varphi)v + (c\theta s\varphi)w \tag{3.78}$$

$$\ddot{x} = \frac{-U_1}{m}(\mathrm{c}\varphi\ \mathrm{s}\theta\ \mathrm{c}\psi + \mathrm{s}\varphi\ \mathrm{s}\psi) \tag{3.79}$$

$$\ddot{y} = \frac{-U_1}{m}(\mathrm{c}\varphi\ \mathrm{s}\theta\ \mathrm{s}\psi - \mathrm{s}\varphi\ \mathrm{c}\psi) \tag{3.80}$$

$$\ddot{z} = g - \frac{U_1}{m}(\mathrm{c}\varphi\ \mathrm{c}\theta) \tag{3.81}$$

$$\dot{\psi} = p + t\theta(qs\varphi + rc\varphi) \tag{3.82}$$

$$\dot{\theta} = qc\varphi - rs\varphi \tag{3.83}$$

$$\dot{\varphi} = 1/c\theta(qs\varphi + rc\varphi) \tag{3.84}$$

$$\dot{p} = \frac{1}{I_{xx}}\ [(I_{xx} - I_{zz})qr + M_x] \tag{3.85}$$

$$\dot{q} = \frac{1}{I_{yy}}\ [(I_{zz} - I_{xx})rp + M_y] \tag{3.86}$$

$$\dot{r} = \frac{1}{I_{zz}}\left[\left(I_{xx} - I_{yy}\right)qp + M_z\right] \tag{3.87}$$

3.7 CONTROLLER DESIGNE AND IMPLEMENTATION

The controllers play a pivotal role in the simulation, serving as the critical components that enable the quadrotor to accurately follow the specified commands. Their importance cannot be overstated, as they directly influence the stability, responsiveness, and overall performance of the quadrotor during flight. A variety of controllers are available for use with quadrotors, each offering distinct advantages and suited for different operational requirements. These include the Linear Quadratic Regulator (LQR), which optimizes performance based on a set of predefined criteria; the Linear Quadratic Gaussian (LQG), which addresses the presence of noise within the system; the Proportional-Integral-Derivative (PID) controller, renowned for its simplicity and effectiveness in a wide range of applications; the H-Infinity controller, designed to achieve robust performance under model uncertainties and external disturbances; and the Sliding Mode Control (SMC), known for its ability to deal with nonlinear dynamics and uncertainties. The selection of a specific controller is crucial, as it must align with the quadrotor's operational context and the objectives of the simulation, ensuring that the quadrotor can achieve the desired performance outcomes with reliability and precision [90].

Utilizing a suitable controller is fundamental, given their critical role in ensuring the effective operation of flight. In this context, the choice to base flight control on a Proportional-Integral-Derivative (PID) controller is strategic. PID controllers stand out for their versatility and robustness, making them an excellent choice for regulating the dynamic behaviours of a quadrotor. This approach enables precise adjustment of flight parameters, such as altitude, orientation, and position, ensuring the quadrotor responds accurately to commands and navigates effectively through its environment. The PID controller's ability to balance the proportional, integral, and derivative components of the flight control system allows for fine-tuned corrections and improvements in stability and responsiveness. This makes it an indispensable tool in the arsenal of flight control techniques, providing a reliable means to achieve enhanced flight performance.

In this part of chapter, we design a control system tailored to the quadrotor's mathematical model, which was elaborated upon in the preceding part of this chapter. Given our objective to track an object accurately, developing a high-performance controller for managing both the attitude and position of the quadrotor is paramount. The designed control system must enable the quadrotor to react swiftly to input commands while minimizing overshoots to maintain precise control. This rapid and controlled response is crucial; without it, the quadrotor could struggle to follow the object's swift movements, potentially resulting in the loss of tracking. Thus, the controller's ability to ensure the quadrotor's agility and precision in its movements is fundamental to achieving successful object tracking.

3.7.1 PID Controller.

The Proportional-Integral-Derivative (PID) controller is a fundamental element in control system engineering, offering a simple yet efficient method for adjusting a system's output to achieve desired performance. This type of controller relies on three key components to modulate the system's behaviour effectively. The Proportional (P) component acts upon the current discrepancy, adjusting the system's output in direct proportion to the gap between the target and actual outputs, ensuring a quick response to changes. The Integral (I) component addresses the cumulative total of past errors, targeting the eradication of any residual steady-state error by integrating the error over time, thus enhancing accuracy.

Lastly, the Derivative (D) component focuses on the error's rate of change, predicting the system's future trajectory. This predictive action aids in mitigating oscillations and enhancing the system's overall stability, making the PID controller a versatile and indispensable tool in the realm of system control [91].

The single proportional controller minimizes the error term by multiplying it with a specific number, but it does not eliminate the steady-state error. To remove this error, past information is needed, and the desired value is generated. An integrator is used to track the past and remove the steady-state error by summarizing the error signal over time. The derivative path predicts future errors and minimizes them, increasing damping in overshoot. Noise, caused by tiny voltage fluctuations, can affect sensor measurements. The derivative gain amplifies high-frequency signals and removes tiny wiggles that impact the system. To do this, a filter is used along with the derivative term to remove these wiggles. The integral and derivative paths work together to minimize the system's overshot and noise [92].

3.7.2 PID Controller for Quadrotor

The PID control system plays a critical role in regulating both the position and orientation of the quadcopter. Central to this setup is the Plant block, which encapsulates a comprehensive mathematical model of the entire system, including the motor mixing algorithm. This crucial block processes input commands to produce the necessary thrust for various operations. Inputs to the motor mixing block are derived from six distinct PID controllers. These controllers receive feedback on the quadcopter's position and orientation directly from the Plant model. They then compare this feedback with the predefined input commands concerning position and altitude. Based on this comparison, the PID controllers adjust and fine-tune the output, generating the precise thrust required to achieve the desired operational state. This sophisticated feedback loop ensures that the quadcopter maintains accurate control over its flight dynamics, enabling it to respond effectively to a wide range of commands and environmental conditions [93].

The proposed model uses six PID controllers in an intelligent way to improve the flight control of the quadcopter. In particular, the altitude controller is committed to reducing any discrepancy in altitude, thus reducing the occurrence of altitude error. In between, the responsibility of fixing errors in roll, pitch, and yaw for the orientation controllers is to guarantee that the quadcopter preserves its specified orientation. Furthermore, the position controller assumes a pivotal function in minimizing the disparity between the intended and realized positions by changing the quadcopter's location with extreme precision in accordance with the target coordinates. The extensive utilization of numerous PID controllers enables precise regulation of the quadcopter's position, orientation, and altitude, which promotes a steady and precise trajectory.

The control system architecture illustrated will serve as the fundamental model for executing our simulations within MATLAB's Simulink environment. This model is composed of six PID controllers that are intricately designed to manage both position and altitude control. The desired trajectory inputs (x_d, y_d, z_d) are processed by the Position Controller to compute the necessary force (F_l), while the orientation inputs (φ_d, θ_d, ψ_d) are managed by the Attitude Controller to determine the appropriate torques (τ_φ, τ_θ, τ_θ). These forces and torques are then passed through the Control Mixing block, which translates them into the individual motor speed commands (ω_1 ω_2 ω_3 ω_4) required to achieve the desired motion. This system effectively integrates the quadrotor's kinematic and dynamic behaviours into a cohesive simulation, enabling precise control over the quadrotor's flight path in response to a predefined trajectory.

Within the Altitude Control block, the target altitude is inputted, prompting the controller to identify any discrepancies between this target and the current altitude, thus creating an error signal. This error signal is then used to adjust the motor thrust accordingly to reach the specified altitude. The control strategy for attitude employs a dual-loop cascade structure. The external loop manages position, while the internal loop regulates the quadcopter's orientation. This strategy is initiated by accepting the preferred position and yaw angle. Initially, any errors in direction are rectified by the yaw controller before these corrections, along with the position inputs, are channelled through the external loop. In the Position block, inputs of yaw and position are utilized to formulate the necessary roll and pitch commands to achieve the target location. These position errors are continuously monitored and corrected to minimize the error to nil. The Attitude Control loop, forming the inner circuit, receives roll and pitch angles from the Position Control as reference signals. These angles are then compared against actual roll and pitch data within the Attitude Controller to address and rectify any deviations from the desired orientation.

As mentioned before, the PID controller features a straightforward structure. displays the block diagram of a basic PID controller within the time domain, we can formulate the controller's equations, which are detailed in equation 3.86.

$$u(t) = K_p \, e(t) + K_I \int_0^t e(\tau) d\tau + K_D \frac{d}{dt} e(t) \quad 3.88)$$

K_p: Proportional Gain.

K_I: Integral Gain.

K_D: Derivative gain.

e(t): The Error Term.

$u(t)$: The Control Input.

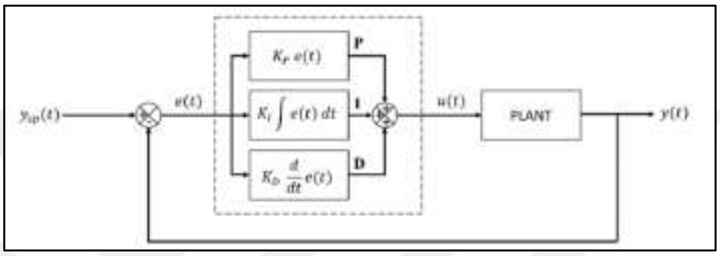

Figure 3.15: Block Diagram of a System with a PID Controller.

Tuning the PID controller involves the adjustment of the K_p K_I and K_D parameters to achieve the desired transient response characteristics of the system's closed-loop transfer function to a unit step input. This ability to finely tune its response based on these three parameters endows the PID controller with a significant advantage, making it a powerful and often preferred choice over other controllers that require more computational resources in many applications. Block diagram of a system with a PID controller

3.7.3 Linearization

The PID control design requires a linear model for tuning purposes. The linearized models help design the controllers via the root locus method and frequency response which gives a better intuition in the control design process. The linearization is done on the principles of small perturbation theory. Additional assumptions need to be made to facilitate the linearization process. Employing the small oscillations assumption proves beneficial in linearizing the quadrotor model. Under this assumption, the sine function simplifies to its argument and the cosine function simplifies to one.

Sabatino (2015) suggests that due to the intricate trigonometric relationships among states, the small angle approximation is employed. This approximation remains valid when the argument is small, aligning with the quadrotor in hover state.

$$\sin(\varphi, \theta, \Psi) \cong (\emptyset, \theta, \Psi) \quad (3.87)$$

$$\cos(\varphi, \theta, \Psi) \cong (1,1,1) \tag{3.88}$$

Neglecting the angles is justified because the product of small angles is close to zero so:

$$\varphi\psi \cong 0\ ;\ \theta\psi \cong 0$$

This assumption will replace them in the linear accelerations below:

$$\begin{bmatrix} \ddot{x} \\ \ddot{y} \\ \ddot{z} \end{bmatrix} = \begin{bmatrix} \frac{-U_1}{m}(\cos\varphi\ \sin\theta\ \cos\psi + \sin\varphi\ s\psi) \\ \frac{-U_1}{m}(\cos\varphi\ \sin\theta\ \sin\psi - \sin\varphi\ \cos\psi) \\ g - \frac{U_1}{m}(\cos\varphi\cos\theta) \end{bmatrix} \tag{3.89}$$

Since g represents the offset for the hover point, we can disregard it in control design and model it in the simulation.

$$\ddot{z} = -\frac{U_1}{m}(\cos\varphi\cos\theta) \tag{3.90}$$

The result will be after replacing the assumption that we established:

$$\begin{bmatrix} \ddot{x} \\ \ddot{y} \\ \ddot{z} \end{bmatrix} = \begin{bmatrix} \frac{-U_1}{m}\theta \\ \frac{U_1}{m}\varphi \\ -\frac{U_1}{m} \end{bmatrix} \tag{3.91}$$

Designating an equilibrium point, often the hovering state where the quadrotor exerts thrust equal to its weight, is crucial for conducting the linearization process. This process simplifies the quadcopter's dynamic equations for control using a PID controller to manage roll, pitch, and yaw movements. Neglecting certain terms reduces modelling complexity during hover, aligning with the small angle approximation's validity for the quadrotor in this state.

Now that we have all the linearized equations of motions about hover point, we can derive a state space model. Let’s first define the state vector of 6 DOF quadcopter system, which can be written as:

$$x = [x\ y\ z\ u\ v\ w\ p\ q\ r\ \varphi\ \theta\ \Psi]^T \tag{3.92}$$

And input vector can be defined as:

$$u = \left[F\ M_x\ M_y\ M_z\ \right]^T \tag{3.93}$$

Now, the state equations can be written as:

$$\dot{x} = Ax + Bu \tag{3.94}$$

$$y = Cx + Du \tag{3.95}$$

And finally, A and B matrices can be constructed as in equations, the state space matrices for A and B can be states as:

$$A = \left.\frac{\partial f\,(x,u)}{\partial x}\right|_{\substack{x=\bar{x}\\ u=\bar{u}}} = \begin{bmatrix} 0 & 0 & 0 & 1 & 0 & 0 & 0 & 0 & 0 & 0 & 0 & 0 \\ 0 & 0 & 0 & 0 & 1 & 0 & 0 & 0 & 0 & 0 & 0 & 0 \\ 0 & 0 & 0 & 0 & 0 & 1 & 0 & 0 & 0 & 0 & 0 & 0 \\ 0 & 0 & 0 & 0 & 0 & 0 & 0 & -g & 0 & 0 & 0 & 0 \\ 0 & 0 & 0 & 0 & 0 & 0 & g & 0 & 0 & 0 & 0 & 0 \\ 0 & 0 & 0 & 0 & 0 & 0 & 0 & 0 & 0 & 0 & 0 & 0 \\ 0 & 0 & 0 & 0 & 0 & 0 & 0 & 0 & 0 & 1 & 0 & 0 \\ 0 & 0 & 0 & 0 & 0 & 0 & 0 & 0 & 0 & 0 & 1 & 0 \\ 0 & 0 & 0 & 0 & 0 & 0 & 0 & 0 & 0 & 0 & 0 & 1 \\ 0 & 0 & 0 & 0 & 0 & 0 & 0 & 0 & 0 & 0 & 0 & 0 \\ 0 & 0 & 0 & 0 & 0 & 0 & 0 & 0 & 0 & 0 & 0 & 0 \\ 0 & 0 & 0 & 0 & 0 & 0 & 0 & 0 & 0 & 0 & 0 & 0 \end{bmatrix} \tag{3.96}$$

$$B = \left.\frac{\partial f\,(x,u)}{\partial u}\right|_{\substack{x=\bar{x}\\ u=\bar{u}}} = \begin{bmatrix} 0 & 0 & 0 & 0 \\ 0 & 0 & 0 & 0 \\ 0 & 0 & 0 & 0 \\ 0 & 0 & 0 & 0 \\ 0 & 0 & 0 & 0 \\ -1/m & 0 & 0 & 0 \\ 0 & 0 & 0 & 0 \\ 0 & 0 & 0 & 0 \\ 0 & 0 & 0 & 0 \\ 0 & 1/I_{xx} & 0 & 0 \\ 0 & 0 & 1/I_{yy} & 0 \\ 0 & 0 & 0 & 1/I_{zz} \end{bmatrix} \tag{3.97}$$

4. RESULTS AND DISCUSSION

This section delves into the outcomes obtained through the utilization of PID controllers in MATLAB and Simulink. Additionally, it elaborates on the application of software and AI tools to analyse data collected from drones, thereby facilitating a comprehensive understanding of our field's health.

4.1 SIMULINK IMPLEMENTATION AND PID RESPONSE ANALYSIS FOR QUADROTOR DRONE TRAJECTORY

4.1.1 Simulink Implementation

The drone's dynamics are analysed by defining its fundamental parameters like weight and moments of inertia, which are crucial for determining its behaviour and control requirements. A detailed table provides all necessary information about the drone's specifications for clarity and reference.

Table 4.1: Parameters of the Quadcopter Designed.

Parameters	**Value**
Ixx	0.09 Kg/m^2
Iyy	0.09 Kg/m^2
Izz	0.15 Kg/m^2
m	8 kg
K	0.0191
Ts	0.01 s

The Simulink diagram representing the quadrotor's design, as depicted in Figure 4.1, is a comprehensive visualization of its control system. It incorporates six PID controllers strategically positioned to regulate various aspects of the quadrotor's behaviour, ensuring stability and responsiveness during flight. Additionally, the trajectory to be followed serves as a crucial reference for the drone's navigation, providing a predefined path for it to track.

Utilizing the mathematical model elucidated in Figure 4.1, the Simulink schematic integrates both position and altitude controllers. These controllers play pivotal roles in guiding the quadrotor along the desired trajectory while maintaining a steady altitude. The position controller governs the drone's lateral movement, ensuring it adheres to the prescribed path accurately. Meanwhile, the altitude controller is responsible for adjusting the drone's vertical position, allowing it to maintain a consistent height above ground level throughout the flight.

The Simulink framework integrates various components to create a robust and versatile quadrotor control system. This approach allows for comprehensive analysis and optimization of the drone's performance, enabling engineers to fine-tune its behaviour and responsiveness to meet specific mission objectives.

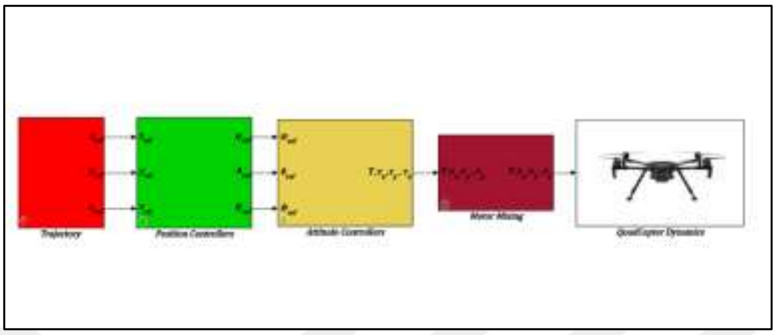

Figure 4.1: Schema of Quadcopter in Simulink.

The trajectory provided is a crucial element in simulating a drone's behaviour, providing insights into its performance in real-world scenarios, especially in agricultural missions. The drone is programmed to ascend to an altitude of 5 meters and navigate along a predefined path, dictating its movement in both x and y directions. The trajectory is defined by the drone's intended flight path, with designated coordinates indicating its movement. For example, the drone is directed to travel 30 meters horizontally along the x-axis for each step and 100 meters along the y-axis, providing a clear trajectory for its mission. This trajectory is essential for understanding the drone's performance in agricultural missions.

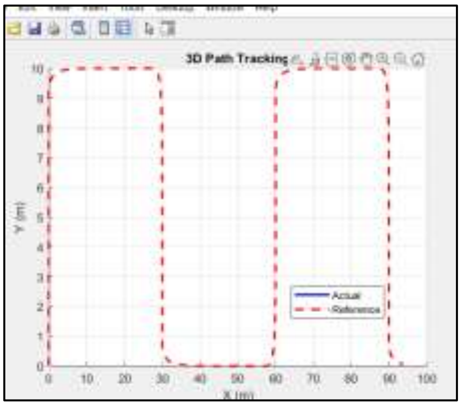

Figure 4.2: Trajectory Given to Follow.

4.1.1.1 Position controllers

The position controller is a critical component of the drone's control system, responsible for maintaining precise positioning in three dimensions: altitude (Z), lateral movement (Y), and forward/backward motion (X). It receives reference inputs, denoted as "Ref Z," "Ref Y," and

"Ref X," representing the desired positions for each dimension. By comparing these reference inputs with the actual positions measured by onboard sensors, the controller calculates deviations, or errors. Utilizing these errors, the position controller generates control signals to adjust the drone's actuators, such as motors and servos, ensuring that the drone manoeuvres effectively to achieve the desired positions.

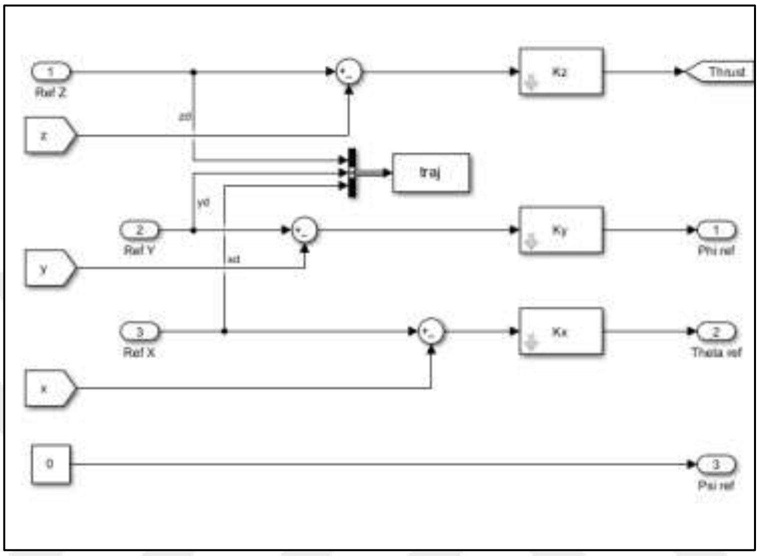

Figure 4.3: Schema Position Controller.

4.1.1.2 Altitude controller

The altitude controller plays a crucial role in maintaining the drone's vertical position, alongside lateral and forward/backward movements. It receives reference inputs for desired positions in each dimension and calculates errors between these desired positions and actual measurements. Utilizing these errors, the controller adjusts the drone's actuators to achieve the desired altitude and ensure stability during flight. Inputs such as thrust and angular adjustments guide the controller's actions, resulting in precise altitude control. Fine-tuning the controller's gains is essential for stable performance and accurate position tracking, optimizing the drone's responsiveness and effectiveness in maintaining altitude and position during flight.

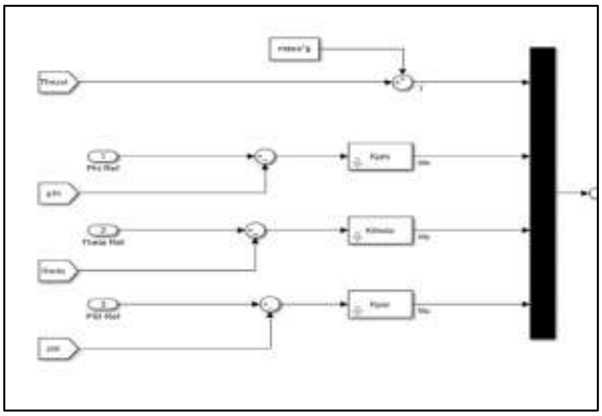

Figure 4.4: Altitude Controller.

4.1.1.3 Motor mixing

Motor mixing is a critical process in multi-rotor drone control, determining the distribution of power among individual motors to achieve desired flight behavior. In drones like quadcopters or hexacopters, motor mixing ensures stability by adjusting motor speeds based on control inputs such as roll, pitch, and yaw. By modulating motor speeds, the drone can execute manoeuvres like tilting, rotating, and maintaining balance. Inputs including desired roll, pitch, and yaw angles influence motor outputs, where each motor receives a specific fraction of the total thrust. For instance, to roll left, motors on the right side accelerate while those on the left side decelerate, facilitating controlled movement. Various motor mixing algorithms, such as "X configuration" or "H configuration", "+ configuration," dictate how motor speeds adjust in response to control inputs and can be customized within flight controllers or firmware. Proper tuning and calibration of motor outputs are essential for stable flight and optimal performance, ensuring level flight and precise control responsiveness.

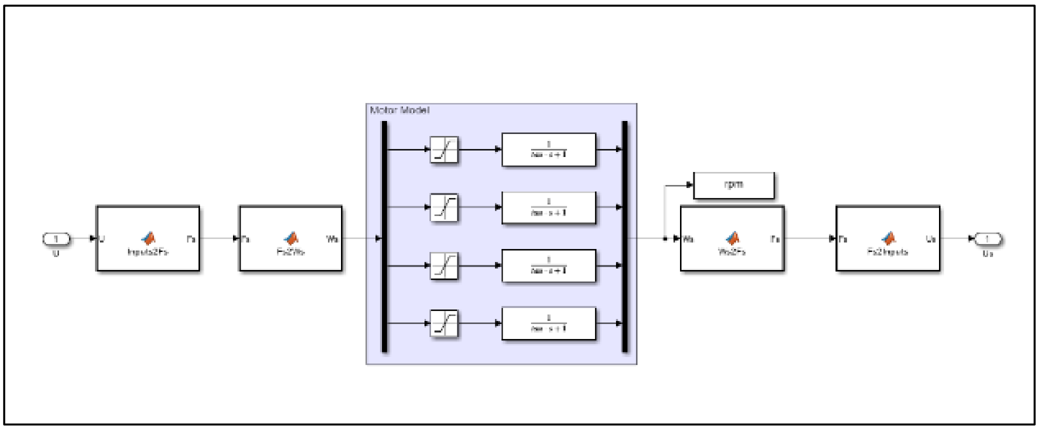

Figure 4.5: Motor Mixing.

4.1.1.4 Quadcopter dynamics

This section, intricately linked to the mathematical model provided earlier, delves into the dynamics of a quadcopter. Input processing, highlighted in red, manages crucial input forces and moments, aligning with parameters outlined in the mathematical model.

The purple section represents the six degrees of freedom (6DOF), encompassing parameters such as velocity, displacement, and Euler angles, all fundamental aspects of the mathematical model. Additionally, output processing, highlighted in red, refines outputs from the 6DOF calculations for integration into control algorithms derived from the mathematical model. This concise depiction underscores the direct relationship between the quadcopter's dynamics and the earlier mathematical model, highlighting its importance in understanding and controlling the quadcopter's flight behaviour.

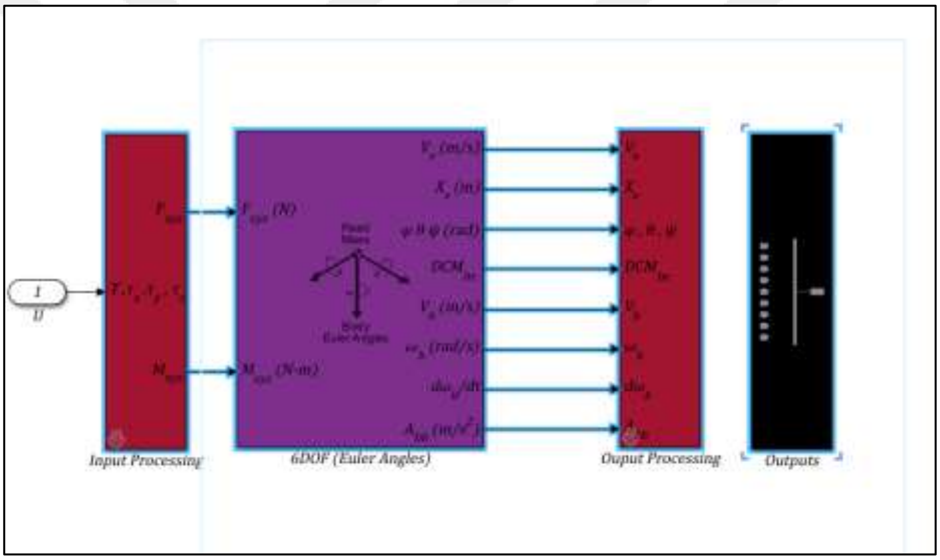

Figure 4.6: Quadcopter Dynamics.

4.1.2 Discussion And Result

In the initial section, we present the results of trajectory tracking for the quadrotor system along the X, Y, and Z axes. This analysis provides insight into how well the quadrotor follows the desired path over time. By comparing the actual trajectory with the reference trajectory, we assess the accuracy and effectiveness of the control system in maintaining the desired flight path. Figures depicting the trajectory tracking performance in each dimension are provided, offering a visual representation of the system's behaviour.

Through this examination, we aim to evaluate the overall performance of the quadrotor system in adhering to the prescribed trajectory and achieving stable flight. The drone trajectory, as depicted in Figure 4.7, outlines the path for the drone's flight.

This trajectory was chosen for simulation, conducted using MATLAB. Figure 4.7 displays the trajectory tracking results, illustrating the comparison between the desired path (in blue) and the actual path followed by the drone (in red).

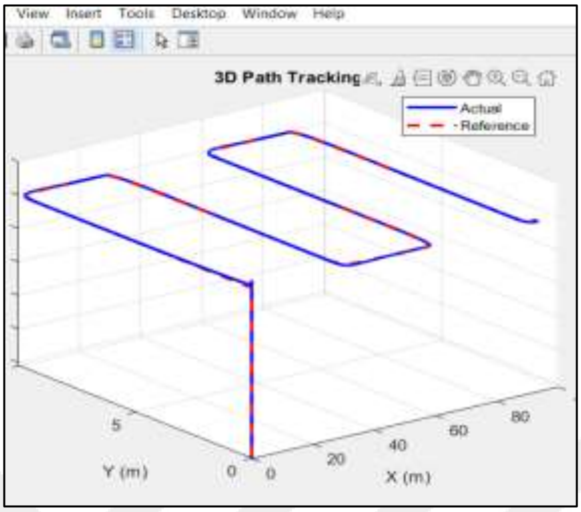

Figure 4.7: The Provided Trajectory is Followed Utilizing a PID Controller.

Figure 4.8 below illustrates the comparison between the reference (in red) and actual (in blue) positions of X, Y, and Z, as well as the yaw pitch and roll angle Figure 4-9, when employing a PID controller.

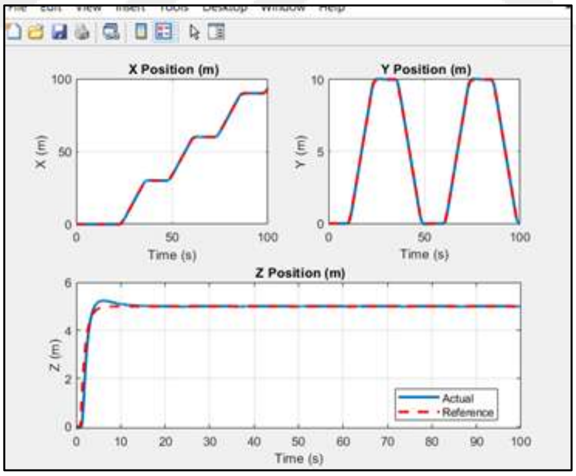

Figure 4.8: Displays the Drone's Trajectory Along the X, Y, and Z axes.

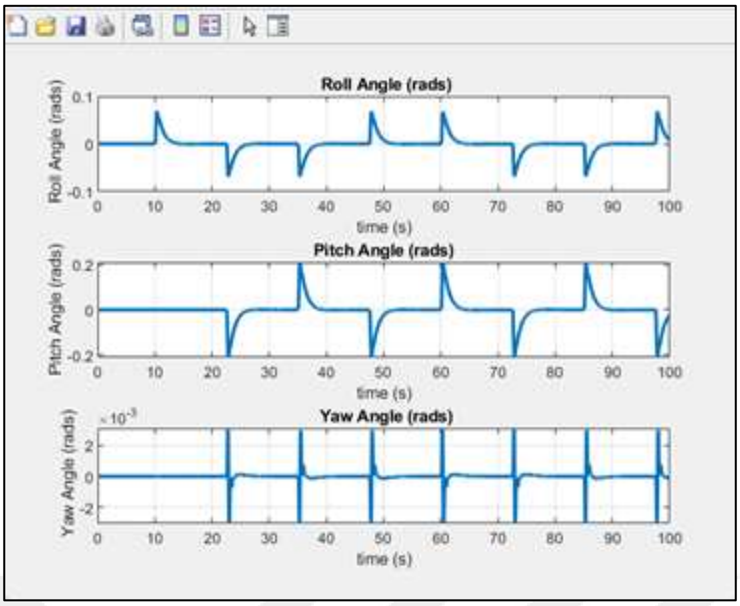

Figure 4.9: Displays the Drone's Trajectory Along the Roll, Pitch, and yaw Angles.

The figure includes three graphs displaying the quadrotor's X, Y, and Z positions over time. Each graph features a solid blue line for the actual position and a dashed red line for the reference position. In the X Position graph, the actual position increases steadily, while the reference position follows a smooth trajectory. Both actual and reference positions in the Y Position graph exhibit oscillatory behaviour. The Z Position graph shows rapid initial growth in the actual position, stabilizing thereafter, contrasting with the constant reference position. These results likely demonstrate the accuracy of the proposed system in comparing the quadrotor's actual trajectory with the desired reference trajectory.

4.1.3 PID Controller Response Analysis

In this section, we delve into the performance evaluation of the PID controllers implemented for trajectory tracking in the quadrotor system. We present the results of trajectory tracking in the X, Y, and Z dimensions, showcasing the effectiveness of the PID controllers in maintaining the desired path. Furthermore, we analyse the performance of each individual controller, highlighting their contributions to the overall trajectory tracking accuracy. Figures are provided to visually demonstrate the performance of the PID controllers, showcasing how the actual trajectory closely follows the desired trajectory. Through this analysis, we aim to assess the efficacy of the PID control scheme in achieving precise trajectory tracking and stable flight behaviour.

Table 4.2: PID Controller Gain Values.

Gain	K_p	K_I	K_D
X	-0.2	-0.01	-0.4
Y	0.2	0.01	0.4
Z	45	10	60
φ	5	1.5	3.5
θ	5	1.5	3.5
ψ	3.5	1.5	2.5

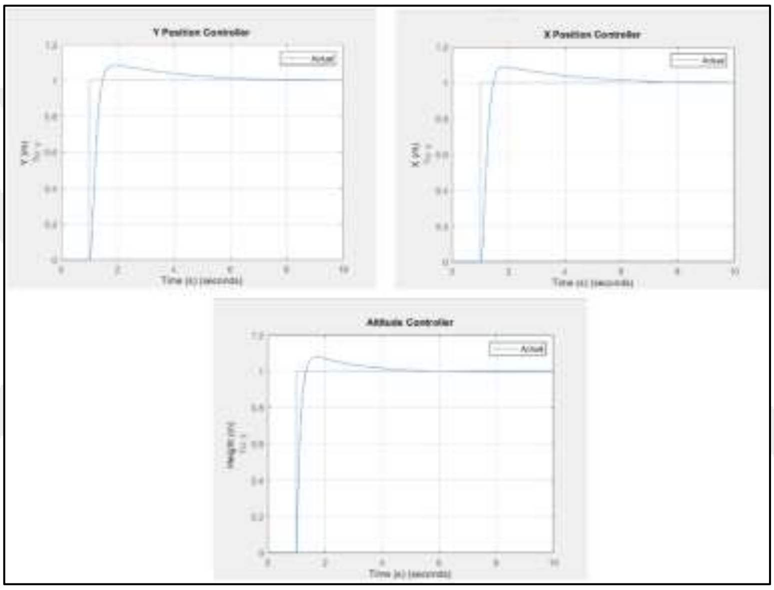

Figure 4.10: Position Step Input Results

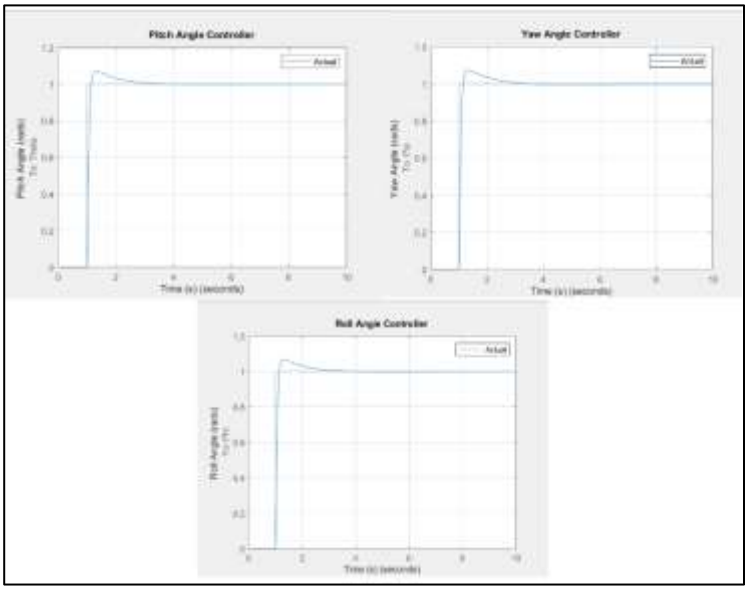

Figure 4.11: Angle Step Input Results.

The tuning of the six parameters—X, Y, and Z for position control, as well as yaw, pitch, and roll for orientation control—aims to ensure stability for the drone throughout its trajectory and flight. By carefully adjusting these parameters within the PID controllers, the system can effectively regulate the drone's position and orientation, minimizing oscillations and deviations from the desired trajectory.

4.2 UTILIZING ADVANCED DATA ANALYSIS AND VISUALIZATION TOOLS FOR PRECISION SPRAYING IN AGRICULTURE

Minimizing the cost of spraying fields poses a significant challenge for farmers in agriculture. The division of costs between chemical products and the expenses incurred in spraying consumes a considerable portion of the budget. Moreover, controlling the field and detecting plant diseases add further complexities. To address these challenges, drones equipped with multispectral cameras are employed to detect plant diseases and transmit the data for analysis. The data is then analysed using Pix4Dfields and Agremo to comprehensively assess the field and explore potential solutions. This study focuses on detecting diseases in crop yields, emphasizing the need for suitable methods in plant disease detection. Additionally, achieving precision in spraying without excessive resource utilization is a key objective of this research. Hence, I have employed Pix4Dfields and Agremo software to demonstrate how they analyse fields and extract results, aiming to enhance precision in agricultural practices.

4.2.1 Analysis Field in Pix4dfield

Pix4Dfields offers a comprehensive platform for agricultural mapping, monitoring, and analysis, but it typically demands more manual input and interaction from the user. While providing extensive capabilities, this software may necessitate additional user intervention and expertise to effectively analyse data. The next stage of our research entails a thorough examination of the field to pinpoint areas needing treatment and to evaluate the general health of the crops. This involves analysing the data captured by the multispectral imagery or RGB camera to identify any potential problems and assess the overall crop condition. For instance, we will focus on identifying weeds and determining where herbicides should be applied to maintain crop health and maximize yield.

Figure 4.12: Example Field Under Examination.

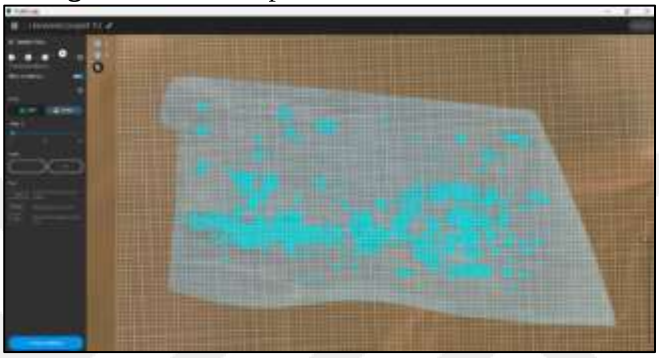

Figure 4.13: Utilizing Pix4Dfields for Weed Detection.

The weed detection process using Pix4Dfields relies on a sophisticated tool that allows users to identify weeds and automatically select all instances of them within the imagery. This tool facilitates the identification of areas requiring herbicide application to maintain crop health and optimize yield.

The final outcome of the weed detection process is illustrated in the figure below, highlighting the specific areas where herbicide application is deemed necessary.

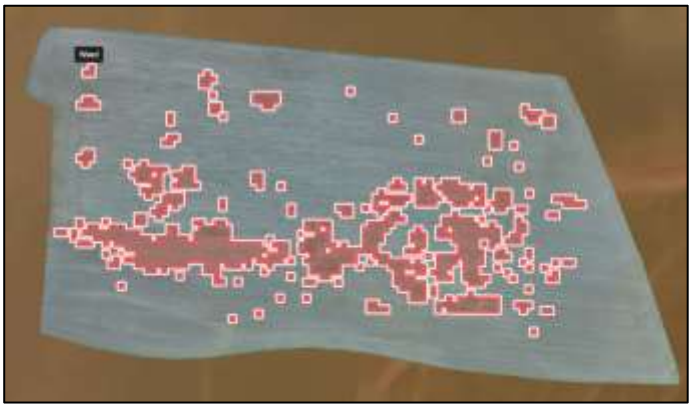

Figure 4.14: Areas Requiring Herbicide Application.

The final crucial step involves achieving pinpoint accuracy in spot spraying. Pix4Dfields facilitates this by enabling you to load your files directly onto the drone within its operational interface. You can save these files in a compatible format for seamless transfer to your drone's SD card, streamlining the process of importing and implementing them for spot spraying tasks. This capability ensures meticulous precision in your agricultural operations, allowing you to target specific areas with utmost accuracy and efficiency.

4.2.2 Analysis Field in Agremo

Agremo is an advanced AI-powered software designed to harness the potential of cutting-edge algorithms and sophisticated image processing techniques. It specializes in the analysis of aerial imagery, enabling users to derive valuable insights and generate precise spraying maps. These maps play a pivotal role in optimizing pesticide application and enhancing overall crop management strategies. In the subsequent steps, we will explore Agremo's capabilities further, with a focus on its effectiveness in Crop Monitoring: Sugar beet field as a prime example of its utility in agricultural applications.

Upon uploading the field data, Agremo's AI-driven platform conducts a comprehensive analysis of the images, leveraging advanced algorithms to detect and identify weeds. The resulting insights provide valuable information necessary for assessing crop health and optimizing agricultural practices. This example underscores the significance of employing advanced tools for precision agriculture, highlighting Agremo's accuracy and efficacy in serving the needs of farmers.

Figure 4.15: Agremo Example.

Figure 4.16: Excess Green Index.

Some of the key results that can be obtained from the analysis include identifying stressed plants, assessing plant Vigor, and detecting waterlogging. These outcomes provide valuable insights into the overall health and status of the crop. By leveraging this information, we can accurately pinpoint areas that require intervention, whether it be for watering or pesticide application. This proactive approach allows for targeted and efficient management of agricultural resources, leading to optimized crop health and yield.

Figure 4.17: Agremo Result of field analysis using.

One of the key results obtained from the analysis using advanced software is the stand count, which provides valuable insights into the density of crops in the field. The figures below illustrate the results obtained from this analysis.

Figure 4.18: Stand Count Result Obtained from Agremo.

Spraying the field after analysing with the Agremo tool provides valuable assistance to users. This tool allows users to identify field variability and stress through plant health monitoring analyses. Additionally, it enables users to create management zones for more targeted spraying operations. By assigning rates and generating prescription files for variable-rate applications, users can optimize their spraying operations. These files are then imported into the controller, allowing the drone to spray only the areas that require treatment, thus minimizing the use of herbicides and ensuring more efficient application.

Demonstrating the impact of this tool in agriculture can be done by comparing the budget costs based on the analysis of the field. We can compare the use of drones versus the use of driving cars for spraying. Additionally, we can compare the area that will be covered using the tools mentioned before and integrate the cost of herbicides or pesticides for spraying. The following table covers this comparison:

Table 4.3: Cost Comparison: Flat Spraying vs. AI and Drone Spraying.

Coste of spraying		
	Flat spraying	DronePix4dfield Agremo
Area sprayed(acres)	65	
Herbicide used per acre	100%	58%
Herbicide cost per acre	7.00$	4.06$
Total herbicide cost	455.00$	263.00$
Yield losses from driving through the field per acre	15.00$	0.00$
Total yield losses from driving through the field	975.00$	0.00$
Total cost	1430.00$	263.00$

The diagram illustrates a comparison of the area required for spraying using conventional flat spraying methods versus drone spraying integrated with AI for analysis. Farmers address fields where drones are unavailable or crops are unhealthy across the entire field, contrary to when utilizing advanced tools.

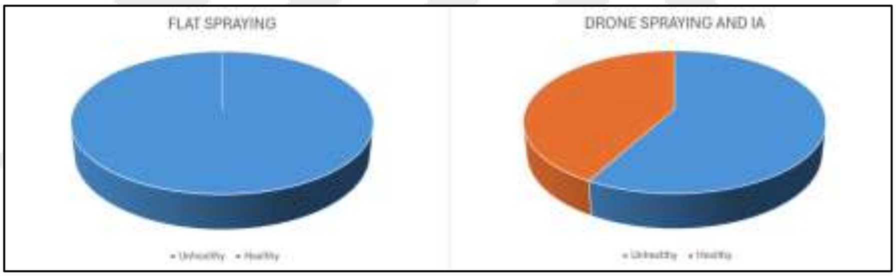

Figure 4.19: Comparison of The Area Required for Spraying.

As farmers I have 500 litter of herbicide need to use it for spraying the field the diagram below shows the usage od herbicides for each case:

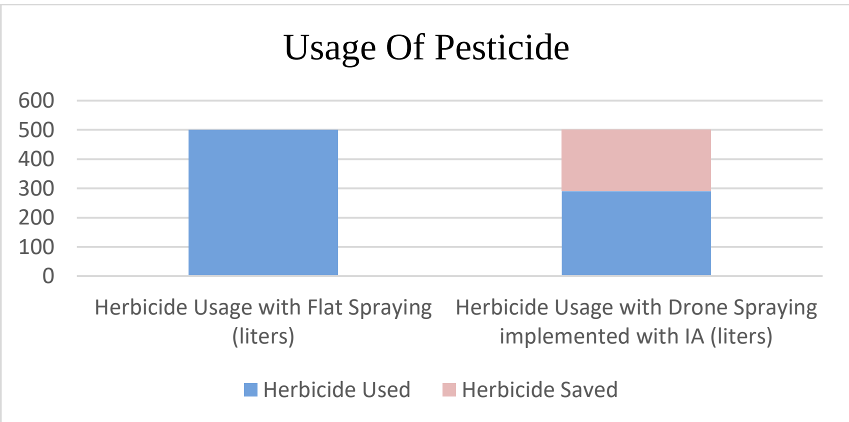

Figure 4.20: Usage of Pesticides for Each Case.

After employing a total of 500 litters of herbicide sprayed using drones integrated with IA technology, there is a reduction of 210 litters compared to the standard herbicide pesticides usage with traditional flat spraying methods.

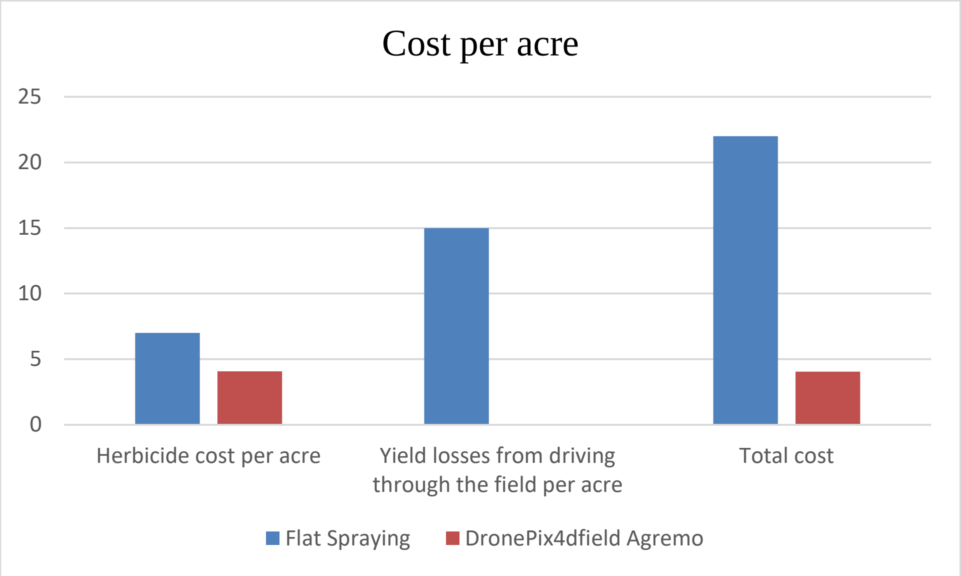

Figure 4.21: Cost Per Acre.

By utilizing drones and advanced tools for weed detection and pinpointing areas requiring spraying, farmers can significantly reduce their costs. For example, the cost per acre decreases from $22 to $4.05. This substantial cost reduction is attributed to the precision targeting enabled by the technology, which minimizes the use of herbicides or pesticides and optimizes resource allocation.

4.3 INTEGRATING SPRAY CONTROL MECHANISMS AND DRONE VISUALIZATION IN MATLAB

After analysing the collected data and identifying areas requiring spraying, the drone requires a mechanism to apply the chemical product or water accurately to specific locations. To achieve this precision, an Arduino and pump system can be utilized. These components will spray the substance based on coordinates received from the controller, ensuring targeted application without wastage.

The pump will receive commands from the Arduino, which in turn receives signals from the flight controller for each predefined point. As the drone navigates to these points, the flight controller instructs the sprayer system to initiate spraying. I have created a small simulation using MATLAB to demonstrate how this process will function.

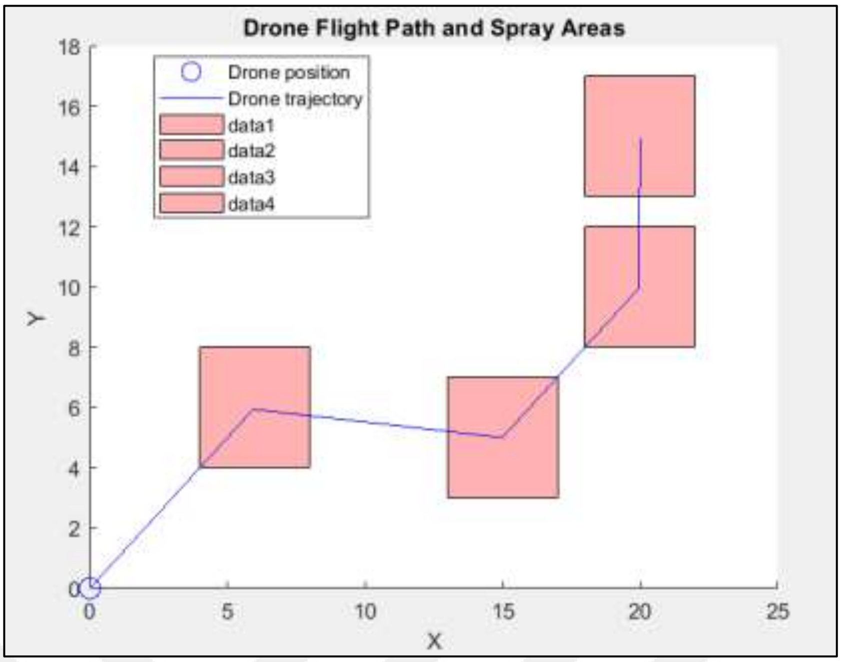

Figure 4.22: Drone Flight Path and Spray Areas.

5. CONCLUSIONS AND FUTURE WORK

In conclusion, this research sheds light on the significance of quadcopter technology in various fields, including agriculture. Drones have revolutionized farming practices by offering efficient solutions to challenges faced by farmers. Specifically, drones designed for agricultural missions provide invaluable assistance by offering precise monitoring, crop spraying, and data collection capabilities. Furthermore, the integration of a multispectral camera will enable data collection regarding the field's health. This data will be analysed using software tools such as Pix4Dfields and Agremo, providing insights into the specific areas requiring spraying.

To address the specific need for a drone capable of spraying pesticides and water over large areas, a quadcopter was meticulously designed using SolidWorks 2022. The quadcopter features a robust frame capable of carrying heavy loads, ensuring durability and reliability during operation. The choice of components, including the TM5212 motor and 15*5CF propeller, was determined through careful consideration of weight-bearing capacity and efficiency. Furthermore, simulations conducted in SolidWorks affirmed the frame's durability and its ability to withstand the demands of agricultural missions. To further validate the performance of this specialized drone, simulations were carried out in MATLAB Simulink, employing PID controllers to assess trajectory tracking and component responsiveness. These simulations provide valuable insights into the drone's capabilities and the effectiveness of the selected components for agricultural missions. Additionally, to further optimize pesticide usage and boost farmers' profits, the drone will utilize a multispectral camera for mapping purposes. This camera will capture data during flight, which will then be analysed using software like PIX4D and AGREMO. These advanced tools enable precise analysis of the collected data, allowing us to identify specific areas in the field that require spraying. By integrating this technology with the drone's capabilities, we can ensure targeted and efficient pesticide application, minimizing waste while maximizing crop health and profitability for farmers.

As the next step, designing a drone capable of continuously accessing pesticides from a ground-based source via a tube presents an innovative solution for agricultural missions. This concept eliminates the need for the drone to return to a central location for refuelling, enhancing its operational efficiency and effectiveness. However, future challenges lie in addressing the issue of flight time, which may become a significant obstacle. To overcome this challenge, a careful balance between an unlimited source of pesticides and extended flight time needs to be achieved. Additionally, integrating swarm drones into the field can further enhance coverage and efficiency, as multiple drones can work simultaneously to cover larger areas and compensate for any individual drone's downtime, ultimately maximizing the utility and impact in the agricultural sector.

REFERENCES

[1] P. Ehrlich and A. Ehrlich, “Can a collapse of global civilization be avoided,” *Proceedings. Biological sciences / The Royal Society*, vol. 280, p. 20122845, Mar. 2013, doi: 10.1098/rspb.2012.2845.

[2] P. Ehrlich and J. Harte, “Opinion: To feed the world in 2050 will require a global revolution,” *Proceedings of the National Academy of Sciences of the United States of America*, vol. 112, pp. 14743–4, Dec. 2015, doi: 10.1073/pnas.1519841112.

[3] P. Balaji, S. Radha, R. Katuri, K. Mareedu, and S. Chennupati, *Design of UAV (Drone) for Crop, Weather Monitoring and for Spraying Fertilizers and Pesticides*. 2018.

[4] C. Lee, S. K. Phang, and H. Mun, “Design and Implementation of an Agricultural UAV With Optimized Spraying Mechanism,” *MATEC Web of Conferences*, vol. 335, p. 02002, Jan. 2021, doi: 10.1051/matecconf/202133502002.

[5] G. Williams, Y. Wang, D. Suman, I. Unlu, and R. Gaugler, “The development of autonomous unmanned aircraft systems for mosquito control,” *PloS one*, vol. 15, p. e0235548, Sep. 2020, doi: 10.1371/journal.pone.0235548.

[6] P. Frankelius, C. Norrman, and K. Johansen, “Agricultural Innovation and the Role of Institutions: Lessons from the Game of Drones,” *J Agric Environ Ethics*, vol. 32, no. 5–6, pp. 681–707, Dec. 2019, doi: 10.1007/s10806-017-9703-6.

[7] P. Kardasz and J. Doskocz, “Drones and Possibilities of Their Using,” *Journal of Civil & Environmental Engineering*, vol. 6, Jan. 2016, doi: 10.4172/2165-784X.1000233.

[8] M. Vaheed, A. Verma, S. Maurya, S. Qidwai, and M. Javed, “Drone Technology-For Smart Agriculture,” 2023, pp. 103–128.

[9] A. Arya and A. E. Perelló, *Management of fungal plant pathogens*. Wallingford: CABI, 2010.

[10] C. Sălceanu, M. Paraschivu, O. Cotuna, V. Sărăţeanu, M. Prioteasa, and I. Flondor, “GLOBAL PESTICIDE MARKET: SIZE, TRENDS, FORECASTS,” vol. 52, pp. 146–157, Jan. 2023, doi: 10.52846/aamc.v52i2.1401.

[11] G. A. Mesías-Ruiz, M. Pérez-Ortiz, J. Dorado, A. I. de Castro, and J. M. Peña, "Boosting precision crop protection towards agriculture 5.0 via machine learning and emerging technologies: A contextual review," *Front. Plant Sci.*, vol. 14, Mar. 2023, doi: 10.3389/fpls.2023.1143326.

[12] F. Akkoyun, "Design and development of an unmanned aerial and ground vehicles for precision pesticide spraying," doctoralThesis, Adnan Menderes Üniversitesi Fen Bilimleri Enstitüsü, 2019.

[13] D. C. Tsouros, S. Bibi, and P. G. Sarigiannidis, "A Review on UAV-Based Applications for Precision Agriculture," *Information*, vol. 10, no. 11, Art. no. 11, Nov. 2019, doi: 10.3390/info10110349.

[14] Karan Kumar Shaw, Vimalkumar. R, and SRM Institute of Science and Technology, "Design and Development of a Drone for Spraying Pesticides, Fertilizers and Disinfectants," *IJERT*, vol. V9, no. 05, p. IJERTV9IS050787, Jun. 2020, doi: 10.17577/IJERTV9IS050787.

[15] G. Borikar, C. Gharat, and S. Deshmukh, "Application of Drone Systems for Spraying Pesticides in Advanced Agriculture: A Review," *IOP Conference Series: Materials Science and Engineering*, vol. 1259, p. 012015, Oct. 2022, doi: 10.1088/1757-899X/1259/1/012015.

[16] H. Nawaz, H. M. Ali, and S.-R. Massan, "Applications of unmanned aerial vehicles: a review," *3C Tecnología*, pp. 85–105, Nov. 2019, doi: 10.17993/3ctecno.2019.specialissue3.85-105.

[17] J. Fan and M. Saadeghvaziri, *Applications of Drones in Infrastructures: Challenges and Opportunities*. 2019. doi: 10.5281/zenodo.3566281.

[18] B. Yudho, M. Heryanto, H. Suprijono, J. Muliadi, and B. Kusumoputro, *Design and development of heavy-lift hexacopter for heavy payload*. 2017, p. 247. doi: 10.1109/ISEMANTIC.2017.8251877.

[19] Spoorthi S., B. Shadaksharappa, Suraj S., and V. K. Manasa, "Freyr drone: Pesticide/fertilizers spraying drone - an agricultural approach," in *2017 2nd International Conference on Computing and Communications Technologies (ICCCT)*, Chennai, India: IEEE, Feb. 2017, pp. 252–255. doi: 10.1109/ICCCT2.2017.7972289.

[20] C. Lum, K. Gauksheim, C. Deseure, J. Vagners, and T. McGeer, "Assessing and Estimating Risk of Operating Unmanned Aerial Systems in Populated Areas," in *11th AIAA Aviation Technology, Integration, and Operations (ATIO) Conference*, Virginia Beach, VA: American Institute of Aeronautics and Astronautics, Sep. 2011. doi: 10.2514/6.2011-6918.

[21] R. Finn and S. Scheding, *Developments and Challenges for Autonomous Unmanned Vehicles: A Compendium*, vol. 3. 2010. doi: 10.1007/978-3-642-10704-7.

[22] V. Boulanin and M. Verbruggen, "Availability and military use of UAVs," 2017, pp. 121–132.

[23] L. Kapustina, N. Izakova, E. Makovkina, and M. Khmelkov, "The global drone market: main development trends," *SHS Web of Conferences*, vol. 129, p. 11004, Jan. 2021, doi: 10.1051/shsconf/202112911004.

[24] H.-W. Choi, H.-J. Kim, S.-K. Kim, and W. S. Na, "An Overview of Drone Applications in the Construction Industry," *Drones*, vol. 7, no. 8, Art. no. 8, Aug. 2023, doi: 10.3390/drones7080515.

[25] S. Sundararaj, K. Dharsan, J. Ganeshraman, and D. Rajarajeswari, "Structural and modal analysis of hybrid low altitude self-sustainable surveillance drone technology frame," *Materials Today: Proceedings*, vol. 37, pp. 409–418, 2021, doi: 10.1016/j.matpr.2020.05.397.

[26] J. Lai, J. Ford, L. Mejias, P. O'Shea, and R. Walker, "Sense and Avoid in UAS: Research and Applications," *Sense and Avoid in UAS: Research and Applications*, pp. 265–294, Apr. 2012, doi: 10.1002/9781119964049.ch10.

[27] L. Ma, M. Li, L. Tong, Y. Wang, and L. Cheng, *Using unmanned aerial vehicle for remote sensing application*. 2013, p. 5. doi: 10.1109/Geoinformatics.2013.6626078.

[28] S. G. Gupta, M. M. Ghonge, and D. P. M. Jawandhiya, "Review of Unmanned Aircraft System (UAS)," vol. 2, no. 4.

[29] R. Sparrow, "Handbook of Unmanned Aerial Vehicles," 2015, pp. 2965–2983. doi: 10.1007/978-90-481-9707-1_98.

[30] U. R. Mogili and B. B. V. L. Deepak, “Review on Application of Drone Systems in Precision Agriculture,” *Procedia Computer Science*, vol. 133, pp. 502–509, 2018, doi: 10.1016/j.procs.2018.07.063.

[31] I. Uyanik and A. Wesley, *Next Generation Gas Emission Monitoring System*. 2019. doi: 10.2118/195015-MS.

[32] C.-H. Lien and S. Vaidyanathan, Eds., *Applications of Sliding Mode Control in Science and Engineering*, 1st ed. 2017. in Studies in Computational Intelligence, no. 709. Cham: Springer International Publishing : Imprint: Springer, 2017. doi: 10.1007/978-3-319-55598-0.

[33] J. Cerro, C. Cruz, A. Barrientos, and J. Rivas, “Unmanned Aerial Vehicles in Agriculture: A Survey,” *Agronomy*, vol. 11, p. 203, Jan. 2021, doi: 10.3390/agronomy11020203.

[34] M. P. Stewart and S. T. Martin, “UNMANNED AERIAL VEHICLES: FUNDAMENTALS, COMPONENTS, MECHANICS, AND REGULATIONS,” *Unmanned Aerial Vehicles*.

[35] M. Bekhti, “Sensors networks : Application to the tracking of moving targets,” 2018.

[36] A. Watts, V. Ambrosia, and E. Hinkley, “Unmanned Aircraft Systems in Remote Sensing and Scientific Research: Classification and Considerations of Use,” *RS*, vol. 4, pp. 1671–1692, Dec. 2012, doi: 10.3390/rs4061671.

[37] G. Brodie, “Chapter 3 - The Use of Physics in Weed Control,” in *Non-Chemical Weed Control*, K. Jabran and B. S. Chauhan, Eds., Academic Press, 2018, pp. 33–59. doi: 10.1016/B978-0-12-809881-3.00003-6.

[38] S. Souvanhnakhoomman, “Review on Application of Drone in Spraying Pesticides and Fertilizers,” vol. 10, pp. 94–98, Dec. 2021, doi: 10.17577/IJERTV10IS110034.

[39] S. Akdan, İ. Öner, N. Akdeniz, A. Bingöl, S. E. Şimşek, and E. Yavsan, “An Agricultural Unmanned Ground Vehicle for Localized Spraying of Harmful Plants Using Convolutional Neural Networks,” 2023. doi: 10.58830/ozgur.pub130.c543.

[40] M. F. A. Jallow, D. G. Awadh, M. S. Albaho, V. Y. Devi, and B. M. Thomas, “Pesticide Knowledge and Safety Practices among Farm Workers in Kuwait: Results of a Survey,” *Int J Environ Res Public Health*, vol. 14, no. 4, p. 340, Apr. 2017, doi: 10.3390/ijerph14040340.

[41] B. S. Faiçal *et al.*, “An adaptive approach for UAV-based pesticide spraying in dynamic environments,” *Computers and Electronics in Agriculture*, vol. 138, pp. 210–223, Jun. 2017, doi: 10.1016/j.compag.2017.04.011.

[42] P. T. Administrator, “Drone Spraying in Agriculture vs Traditional Methods,” TerraTech. Accessed: Oct. 27, 2023. [Online]. Available: https://terratech.ai/comparative-analysis-between-drone-spraying-vs-traditional-methods/

[43] M. Oliver, T. Bishop, and B. Marchant, Eds., “Improving food security through increasing the precision of agricultural development,” in *Precision Agriculture for Sustainability and Environmental Protection*, 0 ed., Routledge, 2013, pp. 52–76. doi: 10.4324/9780203128329-11.

[44] R. Bongiovanni and J. Lowenberg-DeBoer, “Precision Agriculture and Sustainability,” *Precision Agriculture*, vol. 5, pp. 359–387, Aug. 2004, doi: 10.1023/B:PRAG.0000040806.39604.aa.

[45] S. Fountas *et al.*, “Farmer Experience with Precision Agriculture in Denmark and the US Eastern Corn Belt,” *Precision Agriculture*, vol. 6, Apr. 2005, doi: 10.1007/s11119-004-1030-z.

[46] A. Gusev, E. Skvortsov, and V. Sharapova, “The study of the advantages and limitations, risks and possibilities of applying precision farming technologies,” *IOP Conference Series: Earth and Environmental Science*, vol. 949, p. 012019, Jan. 2022, doi: 10.1088/1755-1315/949/1/012019.

[47] V. Gawande *et al.*, “Potential of Precision Farming Technologies for Eco-Friendly Agriculture,” *International Journal of Plant & Soil Science*, vol. 35, pp. 101–112, Aug. 2023, doi: 10.9734/IJPSS/2023/v35i193528.

[48] V. Andreo, *Remote Sensing and Geographic Information Systems in Precision Farming*. 2013.

[49] D. J. Mulla, “Twenty five years of remote sensing in precision agriculture: Key advances and remaining knowledge gaps,” *Biosystems Engineering*, vol. 114, no. 4, pp. 358–371, Apr. 2013, doi: 10.1016/j.biosystemseng.2012.08.009.

[50] S. Apostol *et al.*, “Laser-induced fluorescence signatures as a tool for remote monitoring of water and nitrogen stresses in plants,” *Canadian Journal of Remote Sensing*, vol. 29, pp. 57–65, Feb. 2003, doi: 10.5589/m02-076.

[51] Y. Cohen, V. Alchanatis, M. Meron, Y. Saranga, and J. Tsipris, “Estimation of leaf water potential by thermal imagery and spatial analysis,” *Journal of experimental botany*, vol. 56, pp. 1843–52, Aug. 2005, doi: 10.1093/jxb/eri174.

[52] U. Niethammer, S. Rothmund, M. Joswig, M. James, and J. Travelletti, “UAV-based remote sensing of landslides,” *Int. Arch. Photogramm. Remote Sens. Spatial Inf. Sci.*, vol. XXXVIII Part 5, pp. 496–501, Jan. 2010.

[53] T. Türk Phd, A. Birdal, Ö. Gürsoy, and R. Atun, *INTEGRATION OF UNMANNED AERIAL VEHICLE DATA WITH GEOGRAPHICAL INFORMATION SYSTEMS*. 2018. doi: 10.18509/GBP.2018.65.

[54] A. Laliberte, M. Goforth, C. Steele, and A. Rango, “Multispectral Remote Sensing from Unmanned Aircraft: Image Processing Workflows and Applications for Rangeland Environments,” *Remote Sensing, vol. 3, issue 11, pp. 2529-2551*, vol. 3, pp. 2529–2551, Nov. 2011, doi: 10.3390/rs3112529.

[55] S. Askraba, A. Paap, K. Alameh, J. Rowe, and C. Miller, “Laser-Stabilized Real-Time Plant Discrimination Sensor for Precision Agriculture,” *IEEE Sensors Journal*, vol. 16, no. 17, pp. 6680–6686, Sep. 2016, doi: 10.1109/JSEN.2016.2582908.

[56] A. Paap, S. Askraba, K. Alameh, and J. Rowe, “Photonic-based spectral reflectance sensor for ground-based plant detection and weed discrimination,” *Opt. Express*, vol. 16, no. 2, p. 1051, 2008, doi: 10.1364/OE.16.001051.

[57] F. Ma, M. Yuan, and I. Kozak, “Multispectral imaging: Review of current applications,” *Survey of Ophthalmology*, vol. 68, no. 5, pp. 889–904, Sep. 2023, doi: 10.1016/j.survophthal.2023.06.004.

[58] M. Ghazali, A. Azmin, and W. Rahiman, "Drone Implementation in Precision Agriculture – A Survey," *International Journal of Emerging Technology and Advanced Engineering*, vol. 12, pp. 67–77, Apr. 2022, doi: 10.46338/ijetae0422_10.

[59] A. Bhandari, A. Kumar, and G. K. Singh, "Feature Extraction using Normalized Difference Vegetation Index (NDVI): A Case Study of Jabalpur City," *Procedia Technology*, vol. 6, pp. 612–621, Dec. 2012, doi: 10.1016/j.protcy.2012.10.074.

[60] R. Bischoff and T. Guhl, *Robotic Visions to 2020 and beyond -- The strategic research agenda for robotics in Europe*. 2009.

[61] H. Kasina, M. V. A. R. Bahubalendruni, and R. Botcha, "Robots in Medicine: Past, Present and Future," *International Journal of Manufacturing, Materials, and Mechanical Engineering*, vol. 7, pp. 44–64, Oct. 2017, doi: 10.4018/IJMMME.2017100104.

[62] G. Virk, S. Moon, and R. Gelin, *ISO STANDARDS FOR SERVICE ROBOTS*. 2008, p. 138. doi: 10.1142/9789812835772_0016.

[63] S. Paul, "International Journal of Advanced Research in Computer Engineering & Technology," *International Journal of Advanced Research in Computer Engineering & Technology*, vol. 2, p. 3, Mar. 2013.

[64] S. B, G. Naik, M. R J, P. G. Hedge, and S. K. S. B, "Development of Quad Copter Based Pesticide Spraying Mechanism for Agricultural Applications," *International Journal of Innovative Research in Electrical, Electronics, Instrumentation and Control Engineering*, vol. 5, no. 2, pp. 121–123, Apr. 2017, doi: 10.17148/IJIREEICE/NCAEE.2017.27.

[65] T. S. Kabra, A. V. Kardile, P. R. Bhosale, and A. M. Belekar, "Design, Development & Optimization of a Quad-Copter for Agricultural Applications," vol. 04, no. 07.

[66] D. Yallappa, M. Veerangouda, D. Maski, V. K. Palled, and M. Bheemanna, *Development and evaluation of drone mounted sprayer for pesticide applications to crops*. 2017, p. 7. doi: 10.1109/GHTC.2017.8239330.

[67] M. Ghosal, A. Bobade, and P. Verma, "A Quadcopter Based Environment Health Monitoring System for Smart Cities," *2018 2nd International Conference on Trends in*

Electronics and Informatics (ICOEI), pp. 1423–1426, May 2018, doi: 10.1109/ICOEI.2018.8553686.

[68] A. Goel and P. Aggarwal, “Pesticide poisoning,” *The National medical journal of India*, vol. 20, pp. 182–91, Jul. 2007.

[69] C. P. Shivaji, J. K. Tanaji, N. A. Satish, and P. P. Mone, “AGRICULTURE DRONE FOR SPRAYING FERTILIZER AND PESTICIDES,” vol. 2, no. 6, 2017.

[70] V. Balaska, Z. Adamidou, Z. Vryzas, and A. Gasteratos, “Sustainable Crop Protection via Robotics and Artificial Intelligence Solutions,” *Machines*, vol. 11, no. 8, Art. no. 8, Aug. 2023, doi: 10.3390/machines11080774.

[71] U. R. Mogili and B. B. V. L. Deepak, “Review on Application of Drone Systems in Precision Agriculture,” *Procedia Computer Science*, vol. 133, pp. 502–509, 2018, doi: 10.1016/j.procs.2018.07.063.

[72] H. Guler, H. Zhu, E. Ozkan, R. Derksen, and C. Krause, “Wind Tunnel Evaluation of Drift Reduction Potential and Spray Characteristics with Drift Retardants at High Operating Pressure,” *Journal of ASTM International*, vol. 3, Jan. 2006, doi: 10.1520/JAI13527.

[73] L. S. Pereira *et al.*, “Prediction of crop coefficients from fraction of ground cover and height. Background and validation using ground and remote sensing data,” *Agricultural Water Management*, vol. 241, p. 106197, Nov. 2020, doi: 10.1016/j.agwat.2020.106197.

[74] Y. Alaiwi and A. Mutlu, “MODELLING, SIMULATION AND IMPLEMENTATION OF AUTONOMOUS UNMANNED QUADROTOR,” no. 8, 2018.

[75] M. Walid, N. Slaheddine, A. Mohamed, and B. Lamjed, “Modeling and control of a quadrotor UAV,” in *2014 15th International Conference on Sciences and Techniques of Automatic Control and Computer Engineering (STA)*, Dec. 2014, pp. 343–348. doi: 10.1109/STA.2014.7086762.

[76] M. Uddin, “Cognitive Science and Artificial Intelligence: Simulating the Human Mind and Its Complexity,” *Cognitive Computation and Systems*, vol. 1, Nov. 2019, doi: 10.1049/ccs.2019.0022.

[77] M. Hussain and D. Manhas, “ARTIFICIAL INTELLIGENCE FOR BIG DATA: POTENTIAL AND RELEVANCE,” *International Acadmey of Engineering and Medical Research, 2016*, vol. Volume-1, ISSUE-1, Jan. 2016.

[78] S. K. Phang, C. Cai, B. M. Chen, and T. H. Lee, “Design and mathematical modeling of a 4-standard-propeller (4SP) quadrotor,” in *Proceedings of the 10th World Congress on Intelligent Control and Automation*, Beijing, China: IEEE, Jul. 2012, pp. 3270–3275. doi: 10.1109/WCICA.2012.6358437.

[79] D. Kura, “Brushless Permanent Magnet Motor Design Second Edition”.

[80] C. ESEMEN, *MODELING AND ATTITUDE CONTROL OF A QUADCOPTER USING MODEL PREDICTIVE CONTROLLER*. 2019.

[81] J.-H. Li and P.-M. Lee, “Design of an adaptive nonlinear controller for depth control of an autonomous underwater vehicle,” *Ocean Engineering*, vol. 32, pp. 2165–2181, Dec. 2005, doi: 10.1016/j.oceaneng.2005.02.012.

[82] H. Gao, C. Liu, D. Guo, and J. Liu, *Fuzzy Adaptive PD Control for Quadrotor Helicopter*. 2015. doi: 10.1109/CYBER.2015.7287949.

[83] J. Junkins and M. Shuster, “Geometry of the Euler angles,” *Journal of The Astronautical Sciences - J ASTRONAUT SCI*, vol. 41, pp. 531–543, Oct. 1993.

[84] J. Diebel, “Representing Attitude: Euler Angles, Unit Quaternions, and Rotation Vectors,” *Matrix*, vol. 58, Jan. 2006.

[85] G. G. Slabaugh, “Computing Euler angles from a rotation matrix”.

[86] K. J. Waldron and J. Schmiedeler, “Kinematics,” in *Springer Handbook of Robotics*, B. Siciliano and O. Khatib, Eds., in Springer Handbooks. , Cham: Springer International Publishing, 2016, pp. 11–36. doi: 10.1007/978-3-319-32552-1_2.

[87] M. De Simone, S. Russo, and A. Ruggiero, *Influence of Aerodynamics on Quadrotor Dynamics*. 2015. doi: 10.13140/RG.2.1.5099.3128.

[88] S. FRANCESCO, “Quadrotor control: modeling, nonlinear control design, and simulation,” p. 67, Jun. 2015.

[89] D. Rowell, “Time-Domain Solution of LTI State Equations,” *t e*.

[90] N. Dayana Salim, D. Derawi, S. S. Abdullah, S. A. Mazlan, and H. Zamzuri, “PID plus LQR attitude control for hexarotor MAV in indoor environments,” in *2014 IEEE International Conference on Industrial Technology (ICIT)*, Busan, South Korea: IEEE, Feb. 2014, pp. 85–90. doi: 10.1109/ICIT.2014.6894977.

[91] Hans Oersted and Yudong Ma, “Review of PID Controller Applications for UAVs,” p. 7.

[92] Robert Lacoste, “Chapter 17 - PID Control Without Math,” in *Robert Lacoste’s The Darker Side*, Robert Lacoste, Ed., Boston: Newnes, 2010, pp. 285–304. doi: 10.1016/B978-1-85617-762-7.00017-4.

[93] Yaser Alaiwi and Waleed Altalabani, “Optimized adaptive PID controller design for trajectory tracking of a quadcopter,” 2022.